Science of the Total Environment 898 (2023) 165460

Contents lists available at ScienceDirect

Science of the Total Environment

journal homepage: www.elsevier.com/locate/scitotenv

Spatial distribution of anthropogenic particles and microplastics in a meso-tidal lagoon (Arcachon Bay, France): A multi-compartment approach

Charlotte Lefebvre [a,b,*], Florane Le Bihanic [a], Isabel Jalón-Rojas [a], Edgar Dusacre [a], Lucas Chassaigne--Viscaïno [a], Jeyan Bichon [b], Christelle Clérandeau [a], Bénédicte Morin [a], Sophie Lecomte [b], Jérôme Cachot [a,*]

[a] Univ. Bordeaux, CNRS, Bordeaux INP, EPOC, UMR 5805, F-33600 Pessac, France
[b] Univ. Bordeaux, CNRS, Bordeaux INP, CBMN, UMR 5248, F-33600 Pessac, France

ARTICLE INFO

Editor: Thomas Kevin V

Keywords:
Atlantic coast
Microplastic
Sea surface
Water column
Sediment
Oyster

ABSTRACT

Assessment of microplastic (MP) contamination is still needed to evaluate this threat correctly and tackle this issue. Here, MP contamination was assessed for a meso-tidal lagoon of the Atlantic coast (Arcachon Bay, France). Sea surface, water column, intertidal sediments and wild oysters were sampled. Five different stations were studied to assess the spatial distribution of the contamination. Two were outside of the bay and three were inside the bay (from the inlet to the back). A distinction was made between all anthropogenic particles (AP, i.e. visually sorted) and MP (i.e. plastic polymer confirmed by ATR-FTIR spectroscopy). The length of particles recovered in this study ranged between 17 μm and 5 mm. Concentration and composition in sea surface and water column samples showed spatial variations while sediment and oyster samples did not. At outside stations, the sea surface and the water column presented a blended composition regarding shapes and polymers and low to high concentrations (e.g. 0.16 ± 0.08 MP.m^{-3} and 561.7 ± 68.5 MP.m^{-3}, respectively for sea surface and water column), which can be due to coastal processes and nearby input sources. The inlet station displayed a well-marked pattern only at the sea surface. High AP and MP concentrations were recorded, and fragments along with polyethylene overwhelmed (respectively 76.0 % and 73.2 %). Higher surface currents could explain this pattern. At the bay back, AP and MP concentrations were lower and fibers were mainly recorded. Weaker hydrodynamics in this area was suspected to drive this contamination profile. Overall, fragments and buoyant particles were mainly detected at the sea surface while fibers and negatively buoyant particles prevailed in other compartments. Most of the studied samples presented an important contribution of fiber-shaped particles (from 31.5 % to 94.2 %). Finally, contamination was ubiquitous as AP and MP were found at all stations in all sample types.

1. Introduction

Plastic pollution has been pointed out as a serious and global issue on environmental, aesthetical, economical and societal aspects (Bergmann et al., 2015; Goverse et al., 2014; Moore, 2008). It was estimated that about 4900 million tons of plastic ended in natural environment, corresponding to 60 % of all plastic made until 2015 (Geyer et al., 2017). Plastics were observed in environments considered virgin, such as the arctic sea (Mishra et al., 2021), remote islands (Barnes, 2005) or deep-sea (Chiba et al., 2018). The omnipresence of plastics can induce global threats on marine ecosystems, such as carbon and nutrient cycle impairment or impacts on living organisms (MacLeod et al., 2021). Once released, plastic litter can break down upon several mechanical, chemical or biological processes (Andrady, 2011; Cole et al., 2011) and generate microplastics (MP). Moreover, plastic can be originally manufactured at MP size (GESAMP, 2015). However, the definition of MP is not standardized yet. Frias and Nash (2019) suggested that "*microplastics are any synthetic solid particle or polymeric matrix, with regular or irregular shape and with size ranging from 1 μm to 5 mm, of either primary or secondary manufacturing origin, which are insoluble in water*".

Over the last decade, researchers are putting an increasing effort in order to characterize MP contamination. Hence, MP were detected in all marine compartments such as sea surface (e.g. Panti et al., 2015; Ramírez-Álvarez et al., 2020), water column (e.g. Kanhai et al., 2017; Lefebvre et al., 2019), subtidal sediments (e.g. Claessens et al., 2011), intertidal sediments and beaches (e.g. Bringer et al., 2021; Phuong et al.,

* Corresponding authors at: University of Bordeaux, EPOC UMR 5805 Bâtiment B2, allée Geoffroy Saint-Hilaire, CS50023 33615 Pessac, Cedex, France.
E-mail addresses: charlotte.lefebvre40@gmail.com (C. Lefebvre), jerome.cachot@u-bordeaux.fr (J. Cachot).

https://doi.org/10.1016/j.scitotenv.2023.165460
Received 13 April 2023; Received in revised form 7 July 2023; Accepted 8 July 2023
Available online 16 July 2023

2018a; Tata et al., 2020) or sea ice (e.g. Kanhai et al., 2020; Kelly et al., 2020). The biotic compartment is not spared as a wide range of marine organisms can ingest MP, from zooplankton (e.g. Desforges et al., 2015) to mammals (e.g. Carlsson et al., 2021). The sea surface is one of the most described compartment, which enables the development of numerical models describing the transport of floating MP. It was currently estimated that 51 $\times$ 10^{12} MP are floating at ocean surface (van Sebille et al., 2015). Forecasts for the subtropical convergence zone indicate that MP concentrations will increase by twofold in 2030 and fourfold in 2060 in comparison to the situation of 2016 (Isobe et al., 2019). Microplastics may thus become the pre-dominant non-organic particles among suspended particulate matter (Isobe et al., 2019).

The composition and concentration of MP can be subjected to variabilities at several spatio-temporal scales (Castro et al., 2020; Imhof et al., 2017; Prata et al., 2020). Yet, some aspects of their distribution, dynamic and fate remain unclear. On one hand, these variations can be due to environmental factors such as hydrodynamic features or wind conditions (Balthazar-Silva et al., 2020; Forsberg et al., 2020; Frère et al., 2017; Gündoğdu et al., 2022). In coastal and nearshore waters, behavior of MP can be affected by currents (e.g. tidal-, density-, wind- or wave-driven) or horizontal and vertical mixing for instance (Jalón-Rojas et al., 2019a; Zhang, 2017). On the other hand, anthropogenic factors like closeness and density of anthropic activities can also influence the distribution of MP (Browne et al., 2011; Castro et al., 2020; Jorquera et al., 2022). Additionally, MP vertical and horizontal distributions can be intrinsically linked to their own characteristics such as size, shape or composition (Ballent et al., 2012; Forsberg et al., 2020; Kaandorp et al., 2021). Despite the current growing knowledge, some aspects of MP horizontal and vertical distribution are not yet fully understood.

Formerly, field studies were mostly limited to one or two compartments. More recently, studies included several abiotic matrices, sometimes combined with biotic samples (e.g. Carlsson et al., 2021; Castro et al., 2020; Courtene-Jones et al., 2021; Kazour et al., 2019a). Indeed, a multi-compartment approach can help in understanding MP distribution, their fate or their sources. By including other anthropogenic particles (AP), studies can provide additional information on sources and pathways of the pollution. Here, the term AP is used to refer to manufactured particles, which includes MP particles as well as synthetic, semi-synthetic and dyed particles. This terminology was already applied in different studies on marine abiotic and biotic compartments (e.g. Adams et al., 2021; Collard et al., 2018; Huntington et al., 2020; Klasios et al., 2021). AP can come from the abrasion of textiles, tires, antifouling paints and artificial turfs or abrasive blasting. In particular, cellulosic fibers and rubbery fragments are more and more reported and there are growing concerns about their presence (Arias et al., 2022; Mishra and Rath, 2019; Suaria et al., 2020). Hence, in this study we developed an extended approach by including the analysis of multiple compartments and a detailed description of their contamination by both AP and MP. This approach can help in spotting factors that could influence AP and MP concentrations, compositions, sources, distribution and fate, which are still major scientific questions. Additionally, MP concentrations along with morphometric and polymer types are essential information for ecological risk assessment studies, policy development and mitigation strategies (Bucci and Rochman, 2022; GESAMP, 2019; UNEP, 2021).

Given this overall context, this study aims at presenting a snapshot of AP and MP contamination with an integrated and field-based approach for a complex meso-tidal coastal lagoon, the Arcachon Bay (Atlantic coast of France). The main objectives of this study were to i) characterize composition and concentration of AP and MP in four compartments (i.e. sea surface, water column, intertidal sediments and Pacific oyster – *Magallana gigas*), ii) describe their spatial distribution (horizontal distribution) from the oceanic zone to the back of the bay, and iii) explore potential transport dynamic (vertical distribution) between the studied compartments.

2. Methods

2.1. Studied area

The Arcachon Bay is a coastal lagoon located on the South West coastline of France (44°40′N, 1°10′W; Fig. 1) which is directly connected to the Atlantic Ocean through a tidal inlet (Cayocca, 2001). This mesotidal embayment presents a tide range between 0.8 m at neap tide to 4.5 m at spring tide (Cayocca, 2001). At high tide, it extends over a surface of 174 Km^2 while at low tide about 65 % of its surface emerges (Plus et al., 2009). The hydrodynamics of the bay is primarily driven by semi-diurnal tide cycles, inducing strong water fluxes with the ocean. The mean tidal prism, i.e. volume of water between high and low tide, is estimated at 384 million m^3 for each tidal cycle (Plus et al., 2009). Moreover, the water renewal of the bay can be influenced by freshwater inputs, coming mainly from the Leyre river (Fig. 1), and by winds (Plus et al., 2009). This shallow embayment has a strong irregular bathymetry due to a complex morphology composed of a network of passes, channels and intertidal flats. Currents are stronger at the inlet and in main channels (up to 2 $m.s^{-1}$) while they are weaker in intertidal areas (<0.5 $m.s^{-1}$; Plus et al., 2009). Out of the bay, the oceanic area is exposed to waves (Castelle et al., 2007) and the net annual littoral drift is estimated to 661 million m^3 (Idier et al., 2013).

The Arcachon Bay is affected by several anthropic pressures linked to economical, touristic and demographic aspects. Oyster-farming is emblematic of the region and it constitutes an economically important activity along with spat collection and sales. Oyster farms occupy a surface of 780 ha, managed by 315 oyster firms for an annual production of around 8,000 to 10,000 t in 2013 (SIBA, 2013). There are also professional and recreational fishing activities of different kinds (e.g. vessel, shore fishing, angling). Additionally, aquatic leisure activities in this area include boat ride, sail, jet ski and surf. To support nautical activities, almost 30 harbors and many shipyards are established in the

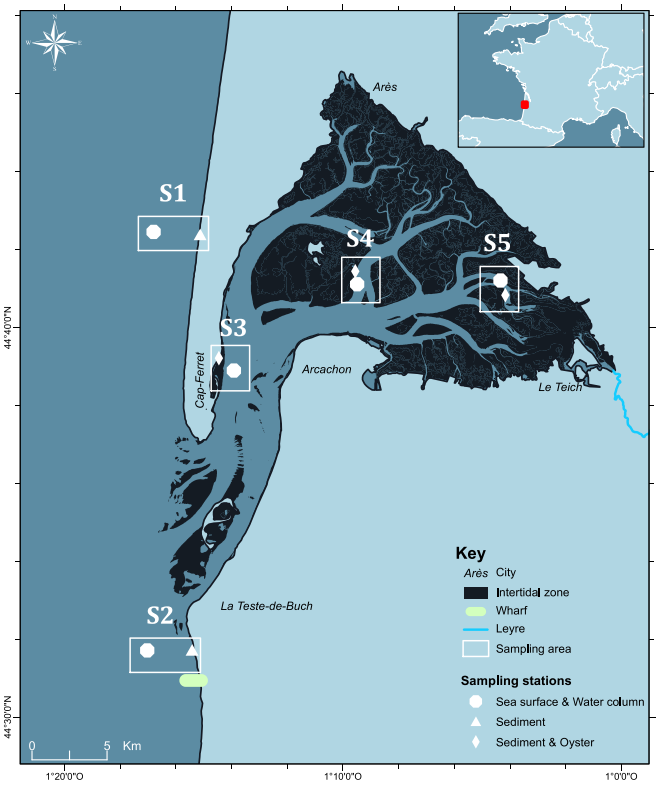

Fig. 1. Studied stations in the Arcachon Bay for sea surface, water column and intertidal sediment samples (from S1 to S5) and for Pacific oyster samples (from S3 to S5). Layers sources: geocean.net and Hydro Carthage.

lagoon, including marina, fishing and oyster-farming harbors (SIBA, 2023). During the touristic season, the bay welcomes over 750,000 people from April to September. Due to the attractiveness of the region, the population is also increasing all year long. Indeed, more than 26,000 new residents moved to the Arcachon Bay between 2008 and 2019 (Institut national de la statistique et des études économiques, 2023). Additionally, effluents from five wastewater treatment plants (four urban plants and one industrial) discharged in the ocean, outside the Arcachon Bay (Fig. 1). The wastewater drainage system has a daily flow of 60,000 m^3 and industrial wastewater contribute to half of this volume. This industry produces paper-based packaging by using pine cellulose from the local forest. Besides, the Leyre River can drain contaminants from agricultural activities into the Arcachon Bay (Tapie and Budzinski, 2018) and could be a source of MP.

2.2. Sampling

Five stations were selected for this study: two in the oceanic area and three inside the bay, from the mouth to the back (Fig. 1). The first oceanic sampling area, named hereafter S1, is located at the North of the Arcachon Bay, either at 2 km offshore or at the sandy beach "*Truc Vert*". This beach is exposed to waves and presents a meso-macrotidal regime. Sediments at S1 beach are primarily composed of medium grained quartz sand (Sénéchal et al., 2009). The second sampling area, named S2, is located outside the bay, either at 2 km offshore or at the sandy beach "*Salie*". Whilst this area is less studied, highly energetic oceanic characteristics reported for S1 are similar at S2. Moreover, the wastewater drainage pipe discharges at the South of the *Salie* beach, near S2. The sampling area of "*Belisaire*", named S3, is located in the North Channel at the inlet of the lagoon. Sediments from the inlet of the bay can be considered as medium sand (Cayocca, 2001; Blanchet et al., 2005). The inlet of the bay is under the influence of strong tidal currents. Besides, this area supports many anthropogenic activities (e.g. oyster-farming, boating, beach use). The sampling area named S4, known as "*L'île aux oiseaux*", is at the center of the bay. "*L'île aux oiseaux*" is a protected natural site of great patrimonial and touristic importance. Sediment is mainly composed of sand (based on the map from Castel et al., 1989). Finally, the last sampling area of "*Branne*", named hereafter S5, is located at the back of the bay in the Audenge Channel. This area receives freshwater inputs from the Leyre River and currents are weaker than at the inlet of the lagoon (0.5 $m.s^{-1}$; Plus et al., 2009). Moreover, sediments can be described as sandy-muddy at the studied site.

Three abiotic sample types and one marine species were collected in April 2019: sea surface, water column, intertidal sediment and Pacific oyster (*Magallena gigas,* previously known as *Crassostrea gigas*, Salvi and Mariottini, 2017; WoRMS Editorial Board, 2023). Abiotic compartments were sampled at all studied stations (S1 to S5) while oysters could be collected only at stations located inside of the bay (S3 to S5, Supp. Mat. 1).

Sea surface was sampled by trawling a manta net (net and cod end net of 300 μm mesh size, 70 cm × 40 cm; ANHYDRE, Hydro-Bios Kiel) equipped with a flowmeter (General Oceanics, 2030 Series). In order to avoid cross-contamination, the net was rinsed with surrounding seawater before each sampling. The top layer of water (about 20 cm) was sampled during 20 min at a vessel speed of around 3 Kn. Geographical positions were recorded at each station (Supp. Mat. 1). The mean volume of filtrated water was 270 ± 76 m^3. After each sampling, the cod end of the net was rinsed thanks to a manual sprayer (Buerkle) filled with filtrated UltraPure water (Elga, PureLab Prima/Maxima). Samples were kept into pre-cleaned glass jars. The sampling was repeated three times at each station with similar boat direction, GPS location, average speed and duration.

Water column samples were collected by using a motor pump (Vilpin Motobomba Plastic-50 Monobloc 2″, max: 40 $m^{-3}.h^{-1}$), with water suction hoses in polyvinylchloride / steel. The motor pump was equipped with a hole suction strainer in stainless steel of 5 mm mesh size. Samplings were taken at 5 m depth except at S5 (3 m depth) and 230 ± 36 L of water were sampled on average. Geographical positions were recorded at each station (Supp. Mat. 1). A homemade filtration system in steel was used in combination with the water pump. It consisted of an assembly of stainless steel sieves with four decreasing mesh sizes (i.e. 5 mm, 250 μm, 125 μm and 50 μm; Fisher Scientific). After the sampling, each sieve was carefully rinsed with manual sprayer filled with filtrated UltraPure water. Rinsing water containing AP and MP from all sieves was gradually transferred into pre-cleaned glass bottles. Except at one site, three replicate samples were made at each station (details in Supp. Mat. 1).

The sampling of intertidal sediments was performed following the protocol developed by the Center of documentation, research and experimentation on accidental water pollution (Cedre) for beach sediment. This standardized protocol is designed for monitoring purposes within the European frameworks (Marine Strategy Framework Directive, 2013). In brief, the transect position at each site was determined before each sampling by checking the hide tide line position for an average tidal range. Starting and ending points of each transect were defined and recorded before the sampling campaign (GPS points and landmarks when possible). Each studied transect was 100 m long and parallel to the water line. The mean tidal range for the different sampling dates was 3.15 ± 0.44 m. The upper 5 cm of sediment was sampled thanks to a stainless steel corer and shovel. Four samplings of 0.25 L each were made within each 25 m long section (see Supp. Mat. 2), and the four sediment samples were mixed in a stainless-steel bowl using a stainless-steel spoon. Then, for each 25 m section, a sub-sampling of 0.30 L was made. These operations were repeated in each 25 m section until the end of the transect (see Supp. Mat. 2). Thus, four sub-samples representing approximately 1.20 L of sediment were collected along the 100 m transect. During the whole sampling process, the operators were placed leeward to avoid contamination from clothes. Moreover, samples were systematically covered with a stainless lid to avoid contamination during the sampling.

Regarding wild Pacific oysters, between 13 and 15 were manually collected at low tide in each site (details in Supp. Mat. 1) and placed in aluminum containers. Pacific oysters were sampled on a pier at S3 and in oyster reefs at S4 and S5.

Abiotic samples were stored at 4 °C and biotic samples were frozen at −20 °C prior analysis.

2.3. Preparation of samples

Sea surface samples were vacuum-filtrated on stainless steel filters of 100 μm mesh size (ø47 mm; HDMI ATOUT METAL). The glass jar containing the sample and the Büchner funnel of the filtration unit was rinsed thoroughly with filtrated UltraPure water to pull the remaining matter onto the filter. The filtration system was rinsed between each sample to avoid cross-contamination. Then, filters were carefully placed into pre-cleaned glass bottles and 150 mL of a 10 % potassium hydroxide (KOH) solution was added in order to partly remove organic matter. Samples were covered with an aluminum foil and organic matter was digested at 50 °C, 180 rpm (IKA RT 15) during 24 h. This procedure was optimized to efficiently digest organic matter and limit the degradation of targeted particles (Dehaut et al., 2016; Treilles et al., 2020). After the digestion of organic matter, samples were again filtrated by following the same procedure.

No digestion or separation was carried out for water column samples as they contained a very low amount of organic matter. They were directly filtrated on stainless steel filters of 50 μm mesh size using the same vacuum filtration system. Glass jars and Büchner funnels were rinsed thoroughly with filtrated UltraPure water.

For the preparation of sediments samples, particles were extracted by means of canola oil, following an adapted protocol from Crichton et al. (2017). The protocol is based on lipophilic properties of MP and was more effective than extraction based on density-separation protocol.

Briefly, sediment samples of each site were separated into four replicates of approximately 300 mL and were placed overnight in an oven at 40 °C. Then, each replicate was weighted and then transferred into a pre-cleaned glass bottle. The mean dry weight of sediments replicates was 368.5 ± 31.3 g. Filtrated UltraPure water and filtrated canola oil were added to the sample (ratio of 20:1:12, *v*/v/v). Then, sediments were vigorously shaken manually during 5 min. After 45 min of sedimentation, the supernatant was vacuum-filtratedonto stainless steel filters of 50 μm mesh size. Glass bottle, funnel of the filtration system and filter were rinsed with a solution of filtrated 96 % ethanol (EtOH) in order to remove stuck particles and oil excess. The extraction was repeated three times for each sample in order to extract the majority of lipophilic particles.

Pacific oysters were defrosted and shells were rinsed with filtrated UltraPure water. The total length (i.e. from the umbo to the top of the shell), the total weight, and the fresh weight of tissue (fw) were recorded for each individual (Ohaus, CS200, scale division: 0.1 g). Mean total lengths of oyster were 9.79 ± 2.01 cm, 8.67 ± 0.93 cm and 8.51 ± 1.31 cm, respectively at S3, S4 and S5. Mean total weights of oysters were 105.05 ± 36.61 g, 101.89 ± 23.57 g and 44.72 ± 16.61 g, respectively at S3, S4 and S5. Oyster's fresh tissues weighed 14.38 ± 6.34 g, 15.81 ± 4.54 g and 6.07 ± 2.77 g, respectively at S3, S4 and S5. Fresh tissues were digested with a 10 % KOH solution (10:1, *v/w*) at 50 °C, 180 rpm for 24 h. The chemical digestion of biological tissues is commonly performed for MP analysis in biotic samples (Dehaut et al., 2016; Kazour et al., 2019a; Phuong et al., 2018b).

After filtration, samples were individually placed in a sealed glass petri dish with a glass cover and they were stored at 4 °C prior to analysis.

2.4. Precautions and control of contamination

From field sampling to chemical analysis, a maximum of precautions was implemented to minimize sample contamination. During sampling and laboratory analysis, pill easy fabrics were avoided and during laboratory analysis, cotton lab coat and nitrile gloves were worn. Solutions of UltraPure water, 70 % ethanol, 96 % ethanol and canola oil were filtrated on a MCE filter of 0.22 μm pore size. The solution of 10 % KOH was filtrated on nylon filter of 0.47 μm pore size to avoid filter deterioration by the KOH solution. All filtrations (e.g. reagents, samples) were done under a clean biosafety cabinet of class 2. ample preparation, transfer of solutions, and sediments settling were also performed under a biosafety cabinet, still to prevent contamination. All materials (e.g. jars, funnel, filtration units, pliers, magnets, Petri dishes, stainless steel filters, glass containers) were rinsed three times with a filtrated solution of 70 % ethanol and then twice with filtrated UltraPure water. Lab benches, biosafety cabinet, stereomicroscope, spectroscope, computer keyboard and all lab devices were also thoroughly cleaned with paper soak with 70 % ethanol. Moreover, the number of people in lab rooms was limited and air conditioner was off.

Additionally, procedural blanks were performed from the laboratory preparation step in order to qualify and quantify background contamination. For both sea surface and water column samples, seven blanks were performed. For intertidal sediments and oyster samples, five and six blanks were respectively performed. Blanks were prepared with the same preparation protocols (digestion, oil extraction and filtration) as their associated type of sample (sea surface, water column, intertidal sediment and Pacific oyster). Furthermore, they were undertaken simultaneously as their associated sample type. Results from statistical analysis showed significantly lower mean abundances in blanks compared to their associated sample type (p-value <0.05 for Pacific oyster and p-values <0.001 for other sample types). As such, the contamination was considered negligible and no correction was applied to raw data. AP and MP characteristics and their mean abundances in procedural blanks, as well as statistical analysis, are detailed in Section 3.1.

2.5. Visual sorting and morphometric characterization

From this step, all studied samples and procedural blanks were analyzed according to the same procedure. Each filter deposit was humidified and placed into a glass petri dish using a stainless-steel blade. Visual sorting of microparticles was made using a stereomicroscope (Leica MZ75; magnification range from ×6.3 to ×50) and a cold light source (Volpi, Intralux 4100). All particles under 5 mm which were suspected to come from anthropogenic sources were extracted. The smallest particle recorded was 17 μm in length. However, particles down to 17 μm were certainly only partly detected and extracted. Each particle was characterized following recommendations of the Marine Strategy Framework Directive (2013). Namely, we recorded the length (i.e. longest dimension), width (i.e. shortest dimension), shape and color of the particle. Six shape categories were recorded in this study: fragment, fiber, film, foam, microbead and rubbery fragment. Visual sorting was primarily guided by criteria reported in Hidalgo-Ruz et al. (2012) and Zhao et al. (2016). Briefly, particles with visible organic structures or cell wall were excluded. We kept particles with unnatural coloration, particles that bring back to shape when pressed, particles that do not brittle after being pressed and fiber-shaped particles with regular thickness that do not break when pressed. All these particles were considered as anthropogenic particles (AP). After characterization and extraction, AP were stored in polystyrene microplates except for sediment samples for which glass vials were used.

2.6. Chemical identification

A sub-sample of 1190 AP (among 4213 AP) was analyzed by Attenuated-Total-Reflectance Fourier-Transform Infrared spectroscopy (ATR-FTIR) using a Nicolet spectrometer (Nexus 870) with Pike technology (MIRacle diamond crystal). The spectrometer was equipped with an MCT detector. The number of AP analyzed in each replicate depended on the number of AP within each shape category (see Supp. Mat. 3). Moreover, the absolute number of AP analyzed was in the range of the recommendations proposed in Kedzierski et al. (2019) in order to obtain a reliable and representative sub-sample of microplastics. In this study, 28 % of all sampled particles were analyzed by ATR-FTIR, which is above the 10 % recommended by the Marine Strategy Framework Directive (2013). The total abundance of extracted and analyzed particles can be found in Supp. Mat. 4. Rubbery fragments were sometimes found in high quantities and their IR spectra were hardly obtainable. As such, they were only analyzed for S2 samples from sea surface and water column and thus chemical identification is not available for rubbery fragments found at another station than S2.

ATR-FTIR spectra were recorded over the 400–4000 cm^{-1} range with a spectral resolution of 4 cm^{-1} (OMNIC software V9.2.98, Thermofisher). An advanced ATR-correction and a manual baseline correction were applied. Then, spectra were matched to different libraries to identify the chemical composition of the particle. Libraries were provided by Thermo Fisher and contained spectra of plastics polymers and/or plastic-related components (e.g. additives, plasticizers, coating). These libraries contain the references of new materials. However, their stay in the ocean impacts the polymers' signature. Thus, we created an environmental library based on manually identified polymers from our samples. In total, each spectrum was compared to 6528 referenced spectra. After comparison, the proposed matching were inspected and a manual validation was made to obtain the polymer identification (e.g. presence and matching of signature absorption bands, recurrence of the listed polymers).

Identified polymers included polyethylene (PE), polypropylene (PP), polystyrene (PS), polyethylene terephthalate (and associated polyester; PET), polyamide (nylon included; PA), a mixture of polyamide and cellulose (PA/CELL), polyacrylic acid (PAA), polyvinyl chloride (PVC), polybutylene terephthalate (PBT), polyoxymethylene (or polyacetal; POM), ethylene-vinyl acetate (EVA), ethylene propylene diene

monomer (EPDM), styrene-butadiene copolymer (SB), Silopren™ (SILIC), cellulose (e.g. cotton, linen, rayon, viscose; CELL) and two additives (MALTRIN M150 and DREWPLUS L-475). As low occurrences were found for PAA, PVC, PBT, POM, EVA, EPDM, SB, SILIC and additives, they were gathered under the category "other" (OTH). When identification was not possible (i.e. low spectra quality or no match assigned), particle's composition was assigned under the category "unknown" (UNK). Furthermore, it has to be underlined that no organic or mineral particles were identified.

2.7. Data treatment and statistical analysis

As only a sub-set of AP was chemically analyzed, MP abundance within each sample replicate was retrieve according to the following calculation (Eq. (1)):

$$MP_{corrected} = Tot_{AP} \times \frac{Tot_{MP}}{Tot_{FTIR}} \quad (1)$$

where $MP_{corrected}$ corresponds to the true abundance of MP in a replicate, Tot_{MP} represents the total amount of MP chemically identified in a replicate, Tot_{AP} corresponds to the number of AP extracted in a replicate, and Tot_{FTIR} represents the abundance of AP analyzed by ATR-FTIR in a replicate.

AP and MP concentrations were calculated by dividing Tot_{AP} or $MP_{corrected}$ abundances by the volume or weight from the corresponding replicate. Additionally, means and standard deviations (SD) were calculated for each station. Additionally, means and SD for the whole studied area (Arcachon Bay) were calculated by considering data at the replicate level (for concentrations and abundances) or at the particle level (for length and width).

All statistical analysis and figures were made thanks to RStudio software (v 2022.07.2; RStudio Team, 2016) and the following packages: car (Fox and Weisberg, 2018), janitor (Firke, 2021), FSA (Ogle et al., 2021), rcompanion (Mangiafico, 2017), rstatix (Kassambara, 2021), ggplot2 (Wickham, 2016), dplyr (Wickham et al., 2021), reshape (Wickham, 2007), scales (Wickham and Seidel, 2020), RColorBrewer (Neuwirth, 2014), hrbrthemes (Rudis, 2020), gridExtra (Auguie and Antonov, 2017) and ggpubr (Kassambara, 2020). Statistical assumptions were validated for AP and MP concentrations in sea surface and water column samples. Indeed, the ANOVA parametric test was performed to analyze spatial variabilities in AP and MP concentrations. The null hypothesis (H0) of similar concentrations between all stations was tested. Then, when significant differences were found between stations, the Tukey honest significance test (HSD test) was performed. Normality and homoscedasticity assumptions in data distribution were not met for AP length nor for AP and MP abundances for all types of samples. Additionally, these assumptions were not gathered for AP and MP concentrations in sediment and wild oyster samples. Thus, the non-parametric test of Kruskall-Wallis (H-test) was performed in order to analyze the spatial variability of these parameters. The null hypothesis (H0) of similar mean length, abundance or concentration was tested for these parameters and samples. When significant differences were found, H-test was followed by the multiple comparison Dunn's test combined with Bonferroni's correction to determine the difference between stations. All significance levels were set at 0.05.

3. Results

This section presents the spatial distribution of AP and MP contamination of the Arcachon Bay in four types of compartments and their associated blanks: sea surface, water column, intertidal sediments and Pacific oysters. The distribution of the contamination is described at five stations, located from the oceanic area (except for Pacific oyster) to the back of the lagoon. The main findings regarding lengths of AP and MP are described for each station and sample type (details in Supp. Mat. 5). The distribution of mean length and mean width by size class are respectively described in Supp. Mat. 6 and Supp. Mat. 5. This section includes shape classification (Figs. 2A, 3A, 4A, 5A, Supp. Mat. 7), color determination (Supp. Mat. 8) and polymer type identification (Figs. 2B, 3B, 4B, 5B, Supp. Mat. 9). Finally, major results about occurrences and mean concentrations of AP and MP are presented in this section (Figs. 2C, 3C, 4C, 5C, D, Supp. Mat. 5).

3.1. Blanks

Mean AP abundance in blanks for water samples was 1.00 ± 1.15 AP per blank and no MP was found. Mean AP length and width were respectively 1.60 ± 1.63 mm and 0.03 ± 0.01 mm (Supp. Mat. 5). There were only fiber-shaped AP (Supp. Mat. 7) that were white (71.4 %), blue or red (both 14.3 %, Supp. Mat. 8). There were mainly made of cellulose (85.7 %), otherwise composition was unknown (14.3 %, Supp. Mat. 9). Mean AP abundances in blank were lower than in sea surface and water column samples (Dunn test, p-values <0.001). In blanks for sediment samples, mean AP and MP abundance per blank was 0.40 ± 0.89. Particles mean length and width were 0.60 ± 0.20 mm and 0.27 ± 0.12 mm, respectively. All particles were red fragments made of PBT (considered in the category OTH, Supp. Mat. 9). Mean AP abundance was lower in procedural blanks than in sediment samples (H-test, p-value <0.001). Blanks for oyster samples displayed a mean abundance of 0.50 ± 1.22 AP per blank and no MP was found. The mean length and width of AP in oyster blanks were not recorded. There were only cellulosic fibers which were either white (66.7 %) or blue (33.3 %). Mean AP abundance was lower than in oyster individual (H-test, p-value = 0.03).

3.2. Sea surface

Overall, fragments and PE were mainly observed at the sea surface and respectively accounted for 49.8 % and 47.9 % of AP (Supp. Mat. 7, Supp. Mat. 9). Mean concentrations at the surface of the Arcachon Bay were 0.15 ± 0.10 $AP.m^{-3}$ and 0.10 ± 0.08 $MP.m^{-3}$ (Supp. Mat. 5).

3.2.1. Size

Mean AP length ranged between 0.92 ± 1.63 mm at S1 and 1.80 ± 1.17 mm at S3 (Supp. Mat. 5). They were not similar between stations (H-test, $N = 691$, p-value <0.001). Indeed, the mean length was higher at S3 than at all other stations (Dunn test, p-value <0.03) and higher at S5 compared to S1 (Dunn test, p-value = 0.03). However, other comparisons showed similar mean length between stations (Dunn post hoc, p-values >0.18). The smallest length of AP was 17 μm and the longest was 4971 μm.

3.2.2. Shape

Fragments were dominant at S2 (39.6 %) and at S3 (76.0 %, Fig. 2A, Supp. Mat. 7). Fibers were mainly detected at S1, S4 and S5, representing respectively 44.5 %, 55.6 % and 78.9 %. In S1 and S4, fragments were the second shape described (at respectively 41.6 % and 33.3 %, Fig. 2A). Rubbery fragments were only recovered at S1 and S2 (12.9 % and 31.6 %, respectively). At S4, 11.1 % of films were observed while negligible proportions were found at other stations (<2 %, Supp. Mat. 7). S2 was the only station where all shapes were described (Fig. 2A, Supp. Mat. 7).

3.2.3. Color

Black AP were mainly found in the two outside stations S1 and S2 (at least 45 %) while white ones were dominant at S3 and S4 (29.6 %; Supp. Mat. 8). At S5, blue AP prevailed (54.4 %). The other colors recorded were blue at S1 and S4, black at S3 and S5 or white at S2, representing between 17.2 % and 37.6 % of all particles.

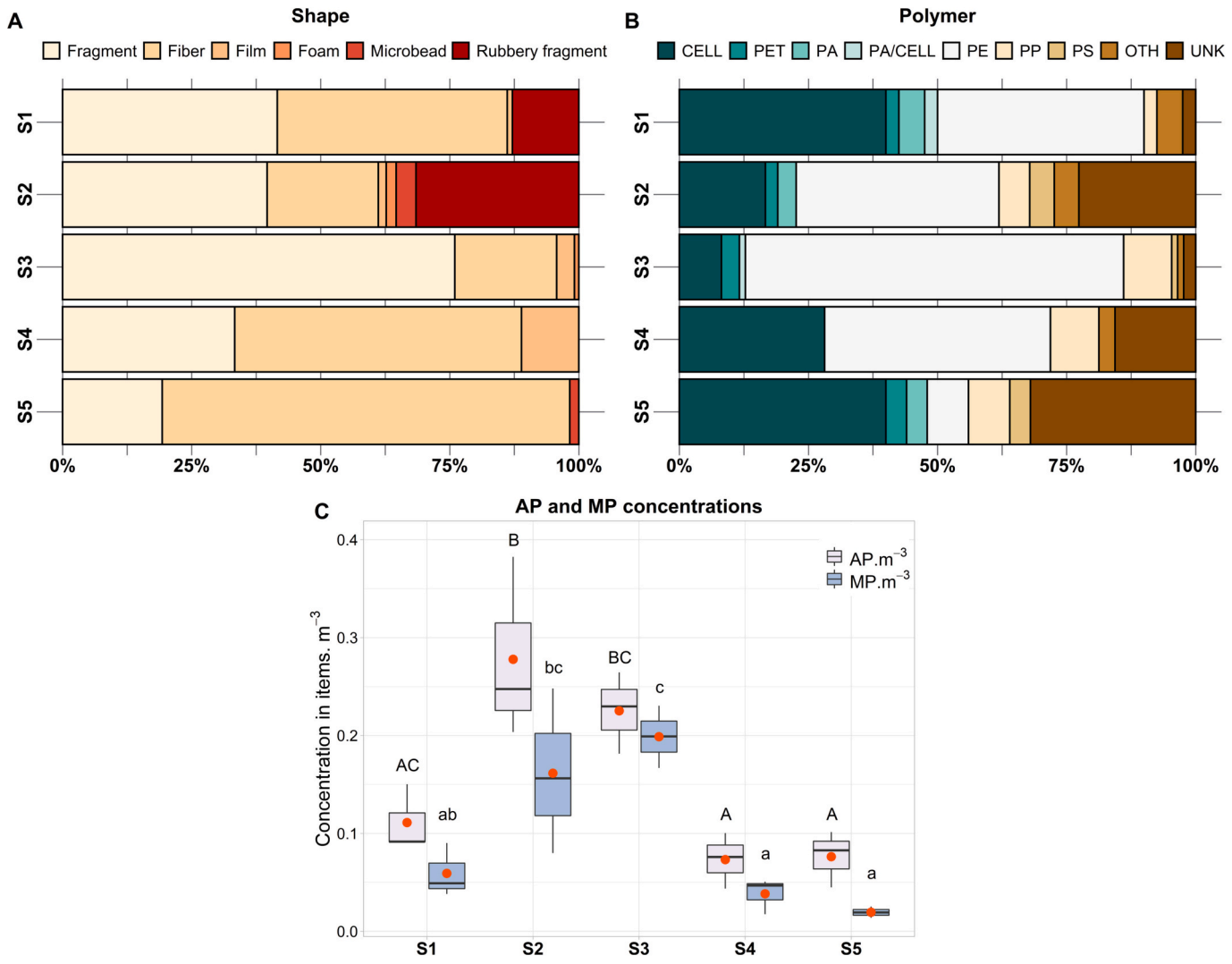

Fig. 2. AP and MP shapes (A, in %), polymer categories (B, in %) and concentrations (C, boxplot, mean concentrations in red points, letters indicate results of the HSD test) at the sea surface.

3.2.4. *Chemical identification*

The same proportion of PE and CELL were found at S1 (40.0 %, Fig. 2B, Supp. Mat. 9). PE prevailed at S2, S3 and S4 (from 39.3 % to 73.2 %) while CELL was mainly observed at S5 (40.0 %). In addition, CELL represented the second polymer at S4 (28.1 %) while it was UNK at S2 and S5 (22.6 % and 32.0 %, respectively). PP was identified at all stations, even though in low proportions (from 2.5 % to 9.4 %).

3.2.5. *Occurrence and concentration of AP and MP*

AP and MP were found at each station and in every replicate. AP concentrations ranged between 0.07 ± 0.03 AP.m^{-3} at S4 and 0.28 ± 0.09 AP.m^{-3} at S2 (Fig. 2C, Supp. Mat. 5). Concentrations of AP showed variabilities between stations (ANOVA, $N = 15$, p-value <0.002). Mean AP concentration at S2 was higher than at S1, S4 and S5 (HSD, p-values <0.02, Fig. 2C). Moreover, mean AP concentrations were higher at S3 than at S4 and S5 (HSD, p-values <0.04). The remaining paired comparisons showed no more differences between stations (HSD, p-values >0.12, Fig. 2C).

MP concentrations ranged between 0.02 ± 0.01 MP.m^{-3} at S5 to 0.20 ± 0.03 MP.m^{-3} at S3 (Fig. 2C, Supp. Mat. 5). There were differences in the mean concentration of MP between some stations (ANOVA, N = 15, p-values <0.02). A higher concentration of MP was found at S3 compared to S1, S4 and S5 (HSD, p-values <0.02). In addition, the mean MP concentration at S2 was higher than at S4 and S5 (HSD, p-values <0.02). Other paired comparisons did not show significant differences (HSD, p-values >0.07).

3.3. *Water column*

Overall, fibers and CELL were mostly encountered in the water column (respectively 55.8 % and 40.2 %, Supp. Mat. 7, Supp. Mat. 9). Mean concentrations in the Arcachon Bay were 952.4 ± 661.3 AP.m^{-3} and 384.0 ± 313.1 MP.m^{-3} (Supp. Mat. 5).

3.3.1. *Size*

The smallest mean length was recorded at S1 (0.48 ± 0.65 mm) while the longest was described at S3 (1.04 ± 0.82 mm, Supp. Mat. 5). Moreover, mean lengths were not similar between stations (H-test, N = 2059, p-value <0.001). Actually, the mean length was lower at S1 than at S2 and both stations displayed lower mean lengths than S3, S4 and S5 (Dunn test, p-values <0.001). No differences were found between mean length from S3, S4 and S5 (Dunn test, p-values >0.19). In the water column, AP lengths ranged from 19 μm to 4888 mm.

3.3.2. *Shape*

Rubbery fragments were predominant at S1 (57.4 %; Fig. 3A) while fibers prevailed at all other stations (from 54.7 to 89.5 %). Fibers were secondly detected at S1 (38.6 %) so were rubbery fragments at S2 and S4

(respectively 38.6 % and 12.7 %). The remaining shape categories proportions were equal or inferior to 5.7 % (Supp. Mat. 7). Additionally, no microbeads were observed in the water column.

3.3.3. Color

Black AP were mainly detected at S1 and S2 (respectively 65.5 % and 45.9 %) while blue AP prevailed at S3, S4 and S5 (from 40.0 % to 53.6 %, Supp. Mat. 8). Blue AP were also notably described at S2 (32.3 %), black one at S4 and S5 (at least 24.8 %) and white one at S3 (19.8 %). The other color proportions were below 16.6 % (see details in Supp. Mat. 8).

3.3.4. Chemical identification

At S2, PET and cellulose were found in similar proportions (26.2 % and 24.5 %, respectively; Fig. 3B). At other stations, cellulosic particles were mainly identified (from 40.4 % to 52.6 %, Fig. 3B). Moreover, PET was the second polymer found at S1 and S5 (respectively 31.2 % and 17.1 %). Unknown polymer category represented between 12.5 % and 21.8 % of AP (Fig. 3B, Supp. Mat. 9). Additionally, PE and OTH accounted for respectively 14.0 % and 7.9 % at S2. Low proportions of PA, PS and PP were found at all stations (from 0.4 % to 9.2 %, Supp. Mat. 9).

3.3.5. Occurrence and concentration of AP and MP

AP and MP were found at all stations and even in every replicate (Supp. Mat. 4). Concentrations of AP in the water column ranged between 338.7 ± 260.2 AP.m^{-3} at S3 and 1994.4 ± 162.0 AP.m^{-3} at S1 (Fig. 3C, Supp. Mat. 5). Significant differences in mean AP concentrations were noticed between stations (ANOVA, $N = 13$, p-value <0.001). Higher mean concentration was found at S1 compared to all other stations (HSD, p-values <0.01). Other comparisons between stations did not display significant differences for AP mean concentrations (HSD, p-values >0.05).

The concentration of MP was minimal at S3 (102.1 ± 102.3 MP.m^{-3}) and maximal at S1 (842.7 ± 168.4 MP.m^{-3}, Fig. 3C, Supp. Mat. 5). Mean MP concentrations showed significant differences between stations (ANOVA, N = 13, p-value <0.001). Indeed, mean concentration was higher at S1 than at S3, S4 and S5 (HSD, p-values <0.01). Moreover, the mean concentration of MP at S2 was higher than at S3 and S4 (HSD, p-value <0.04). Other comparisons between stations displayed no significant differences (HSD, p-value >0.05).

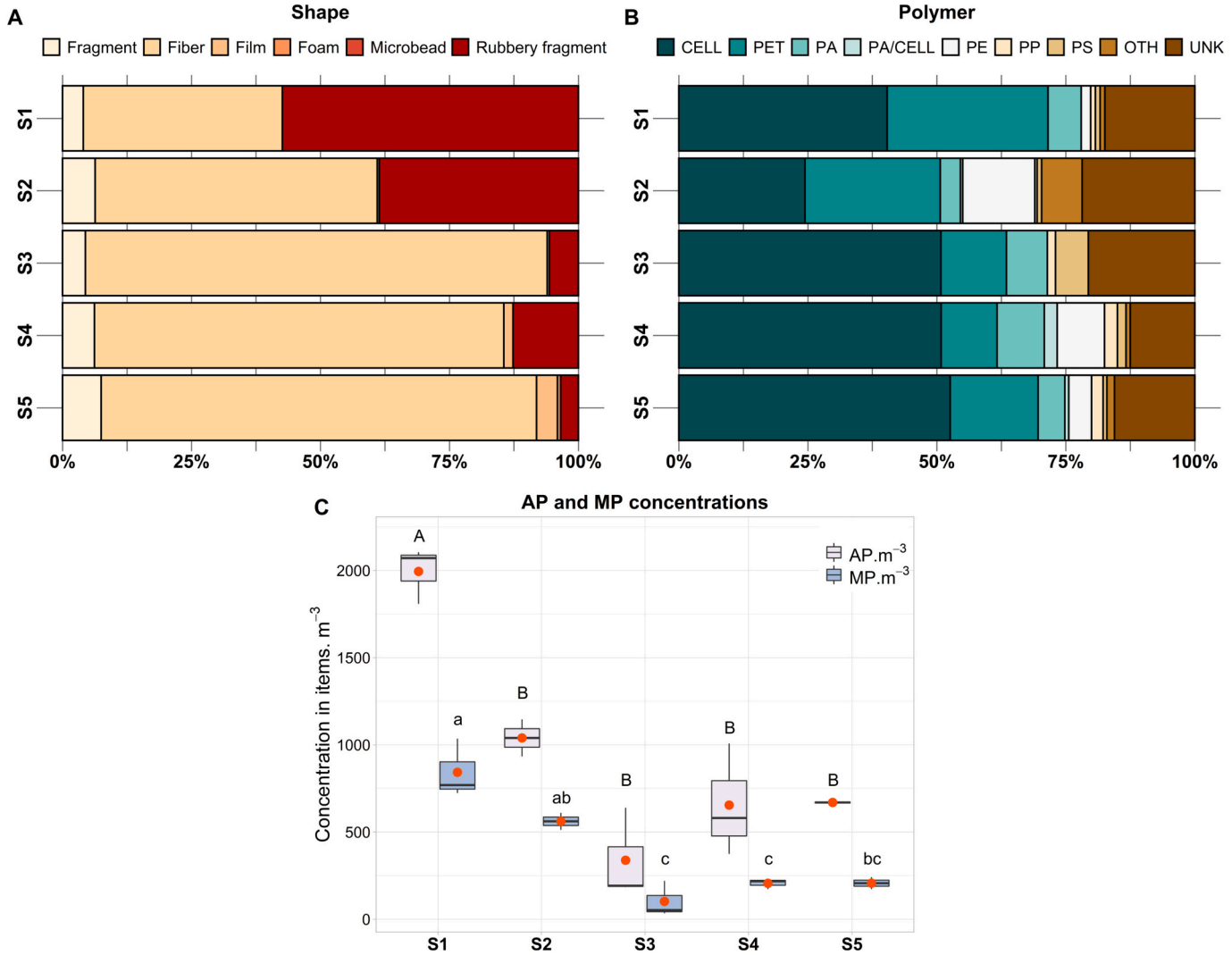

Fig. 3. AP and MP shapes (A, in %), polymer categories (B, in %) and concentrations (C, boxplot, mean concentrations in red points, letters indicate results of the HSD test) in the water column.

3.4. Intertidal sediment

In sediments, fibers and CELL overwhelmed, representing respectively 94.4 % and 69.9 % of all AP (Supp. Mat. 7, Supp. Mat. 9). Mean concentrations in intertidal sediments of the Arcachon Bay were 40.10 ± 33.40 AP.kg^{-1} and 6.91 ± 9.25 MP.kg^{-1} (Supp. Mat. 5).

3.4.1. Size

The lowest mean length was observed at both S3 (1.15 ± 0.79 mm) and S5 (1.15 ± 0.97 mm) and the highest at S4 (1.80 ± 1.00 mm, Supp. Mat. 5). Comparisons between stations indicated significant differences (H-test, $N = 291$, p-value <0.001). Indeed, a longer mean length was found at S4 compared to S1, S3 and S5 (Dunn test, p-values <0.01). Moreover, mean length was higher at S2 than at S3 and S5 (Dunn test, p-values <0.04). Other comparisons between stations did not show significant differences (Dunn test, p-values >0.14). Additionally, the smallest AP was 114 μm in length and the longest was 4393 μm.

3.4.2. Shape

At each station, fiber-shaped AP were overwhelming (from 85.7 % to 97.8 %) while low proportions of fragments were observed (from 1.2 to 9.5 %, Fig. 4A). Films were absent at S3 and were encountered in low proportions at all other stations (from 1.2 % to 4.8 %). No rubbery fragments, foams, or microbeads were observed in sediment samples (Supp. Mat. 7).

3.4.3. Color

AP were mainly blue at all stations (from 60.0 % to 80.0 %). White particles represented 16.5 % and 19.5 %, respectively at S2 and S4. Red ones constituted respectively 14.5 % and 12.1 % of all recorded colors of AP at S3 and S5. Additionally, green AP were recorded at 17.6 % at S4. Regardless of the station, other color proportions were lower than 10 % (Supp. Mat. 8).

3.4.4. Chemical identification

Cellulose was the main polymer found regardless of the station (from 57.1 % to 83.8 %, Fig. 4B). PET and PE were the second polymers identified at S1 (both 6.9 %). Proportions of UNK and PET at S4 were respectively 15.2 % and 10.9 %. At S5, the UNK category accounted for 35.7 %. No PP or PS particles were found in intertidal sediment samples (Supp. Mat. 9).

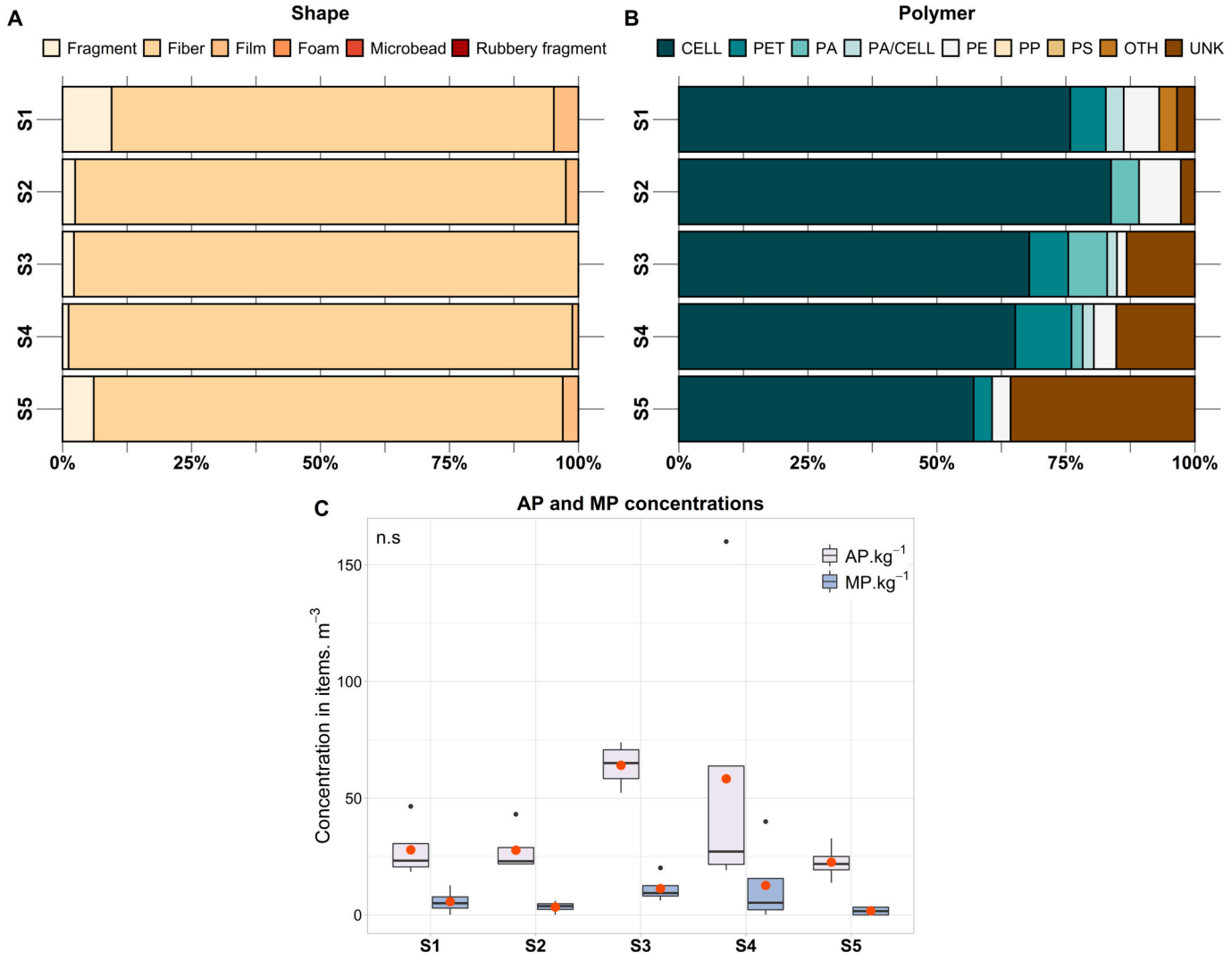

Fig. 4. AP and MP shapes (A, in %), polymer categories (B, in %) and concentrations (C, boxplot,mean concentrations in red points, n.s indicates non-significant result in H-test) in intertidal sediments.

3.4.5. Occurrence and concentration of AP and MP

AP were found at all stations and in all replicates while MP were detected at all stations and in 75 % of replicates. AP concentrations ranged from 22.55 ± 7.81 AP.kg^{-1} at S5 and 64.08 ± 9.68 AP.kg^{-1} at S3 (Fig. 4C, Supp. Mat. 5). Mean AP concentrations showed no significant differences between stations (H-test, $N = 20$, p-value = 0.09).

MP concentrations ranged from 1.71 ± 1.99 MP.kg^{-1} at S5 and 12.59 ± 18.52 MP.kg^{-1} at S4 (Fig. 4C, Supp. Mat. 5). However, mean MP concentrations were not different between stations (H-test, N = 20, p-value = 0.11).

3.5. Pacific oyster

Overall, fibers and cellulose overwhelmed in Pacific oysters, representing respectively 89.4 % and 56.4 % (Supp. Mat. 7, Supp. Mat. 9). Overall mean concentrations in Pacific oyster were 0.33 ± 0.50 AP.g^{-1} fw (or 2.42 ± 2.50 AP.indiv^{-1}) and 0.13 ± 0.26 MP.g^{-1} fw (0.94 ± 1.56 MP.indiv^{-1}; Supp. Mat. 5).

3.5.1. Size

Regarding mean AP length, they ranged between 1.31 ± 0.93 mm at S3 and 2.29 ± 1.32 mm at S5 (Supp. Mat. 5). No significant differences were found in mean lengths between stations (H-test, $N = 62$, p-value = 0.05). The smallest AP length recorded was 211 μm while the longest one was 4917 μm.

3.5.2. Shape

Fiber-shaped AP were particularly dominant in all sampled stations (from 82.0 % to 96.4 %; Fig. 5A). Yet, fragments, films and foams were recorded at S5, representing 12.0 %, 4.0 % and 2.0 % of all AP, respectively. Fragments were found at S3 and films at S4 even though their proportions were lower than 4.0 %. No microbeads or rubbery fragments were detected in individuals of Pacific oyster (Supp. Mat. 7).

3.5.3. Color

The main color recorded was blue at S3 (53.9 %) while it was white at S4 and S5 (at least 46.0 %). White AP were secondly described at S3 (26.9 %) while it was blue AP at S4 and S5 (at least 17.9 %). Moreover, green particles represented 14.0 % of all AP at S4. Despite in low proportions, black AP were identified at all stations (at least 7.1 %), as well as pink AP (at least 2.0 %, see Supp. Mat. 8 for details).

3.5.4. Chemical identification

Cellulosic particles were mainly detected whatever the station (from 47.4 % to 61.1 %; Fig. 5B). The second most common polymer was PET at S3 (21.0 %), PA and PE at S4 (both 11.1 %) and PA/CELL at S5 (24.0

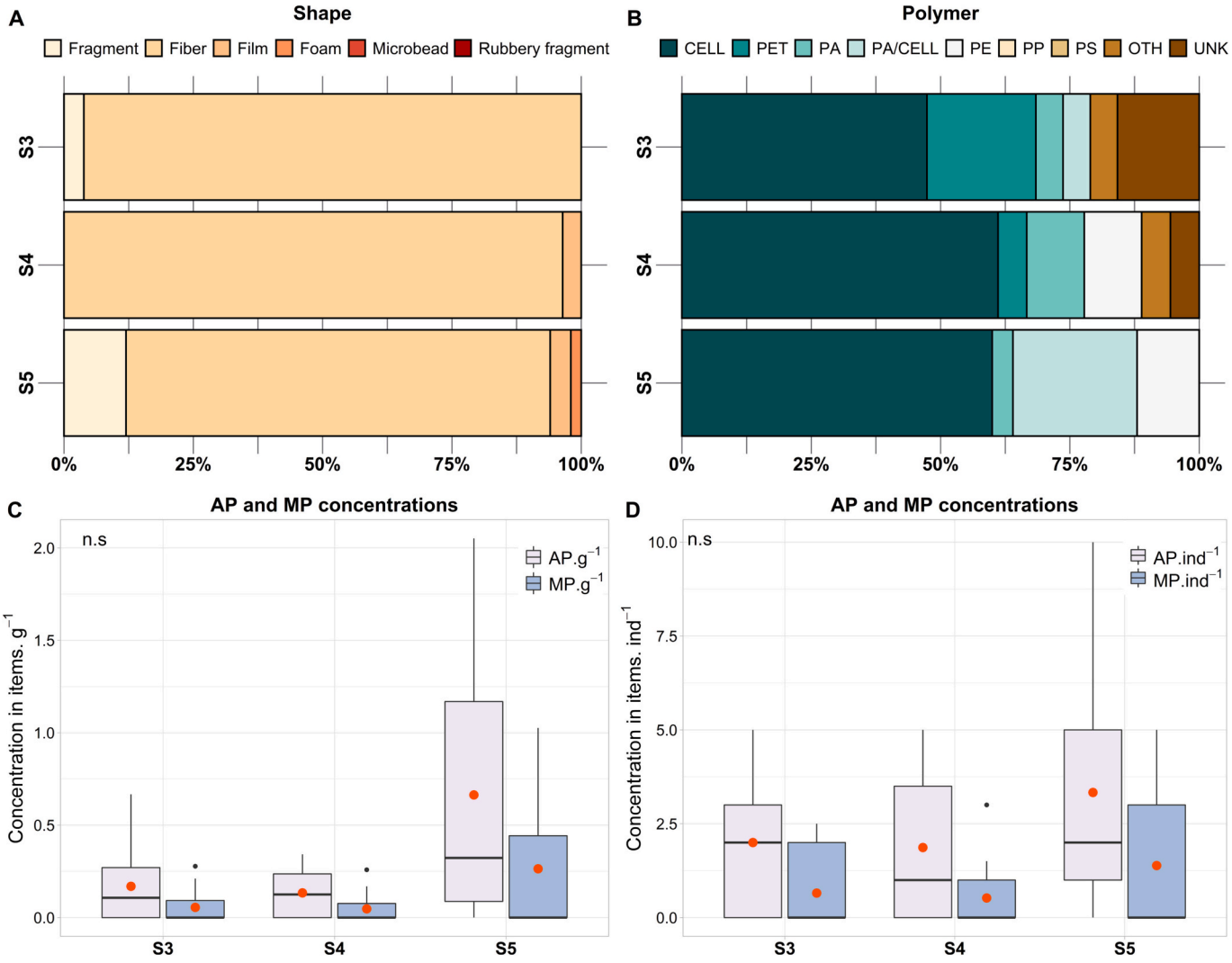

Fig. 5. AP and MP shapes (A, in %), polymer categories (B, in %), concentrations per gram of fresh weight (C, boxplot, mean concentrations in red points, n.s indicates non-significant result in H-test) and abundance per individual (D, boxplot, mean concentrations in red points, n.s indicates non-significant result in H-test) in wild Pacific oysters.

%). Additionally, PE represented 12.0 % of all polymers at S5 (Fig. 5B). Unknown polymers represented 15.8 % at S3, 5.5 % at S4 and 0.0 % at S5. Other proportions of polymers were lower than 5.6 %. PP and PS were not detected in oyster samples (Fig. 5B, Supp. Mat. 9).

3.5.5. Occurrence and concentration of AP and MP

AP were found in 75.0 % of oysters while MP were found in 34.8 % of individuals (Supp. Mat. 4). The concentration of AP per gram (fw) ranged between 0.13 ± 0.13 AP.g^{-1} at S4 and 0.66 ± 0.73 AP.g^{-1} at S5 (Fig. 5C, Fig. 5D, Supp. Mat. 5). These values correspond to a number of AP per individual of 2.00 ± 1.96 AP.ind^{-1}, 1.87 ± 1.81 AP.ind^{-1} and 3.33 ± 3.29 AP.ind^{-1}, respectively at S3, S4 and S5. There were no significant differences between stations regarding both AP concentration units (per gram or per individual; H-test, $N = 43$, p-values >0.07).

MP per gram of fresh weight ranged between 0.05 ± 0.08 MP.g^{-1} at S4 and 0.26 ± 0.40 MP.g^{-1} at S5 (Fig. 5C, Fig. 5D, Supp. Mat. 5). These values correspond to concentration of MP per individual of 0.85 ± 1.52 MP.ind^{-1}, 0.59 ± 0.96 MP.ind^{-1} and 1.39 ± 2.00 MP.ind^{-1} at S3, S4 and S5. No significant differences between stations were found for mean MP concentrations regardless of the unit (H-test, N = 43, p-values >0.49).

4. Discussion

4.1. Sea surface

A mix of several representative shapes and polymers was described at the two outside stations (S1 and S2) at the sea surface. Samples were mainly composed of fragments, fibers and rubbery fragments along with PE, CELL and UNK polymers. In comparison with all the studied stations, AP and MP concentrations varied from moderate to high at the two outside stations. Moreover, higher AP concentrations were found at the southern outside station (S2) compared to the northern one (S1). Wastewater treatment plant (WWTP) effluents discharging nearby S2 could play a role in the important concentrations of AP and MP found at outside stations, in particular at S2. Indeed, WWTP effluents are a well-known source of AP and MP in the aquatic environment (Kazour et al., 2019b; Parker-Jurd et al., 2021), which contributes to the contamination of nearby coastal waters. As well, the proximity with effluents discharge point may have contributed to the mix of shape and polymers found at S1 and S2, and to the important diversity of shape found at S2. Moreover, this coastal area can be exposed to a high energy oceanic environment and important longshore drift (Castelle et al., 2007; Idier et al., 2013) which could impact the behavior of particles by generating important water mixing. As well as the above-mentioned potential influence of the WWTP outflow, environmental conditions could partly explain the mixed composition and the variable concentrations found at outside stations.

On another note, a non-negligible proportions of rubbery fragments and unknown polymers were found at S2. They presented a very irregular shape with numerous rounded borders, deep dark coloration and rubbery texture. Polymer identification was technically difficult for these particles as black carbon interferes with IR spectra. Indeed, black carbon absorbs and scatters IR light, which makes polymer identification very challenging (Eisentraut et al., 2018; Leads and Weinstein, 2019). Nonetheless, they are likely to come from the wear and tear of tires which are known to release particles into the environment (Boucher and Friot, 2017; Kole et al., 2017). These particles can enter the ocean by atmospheric depositions, runoffs and WWTP outfall (Parker-Jurd et al., 2021). Moreover, it was also suggested that they could be generated by nautical activities (Bråte et al., 2020; Lusher et al., 2017). The presence of this type of particle at outside stations suggests that ocean-based sources, such as nautical activities and WWTP drainage, are the most likely ones.

Regarding the station at the inlet of the bay (S3), a singular profile of contamination was observed. Mean AP length and width were the highest, length classes from 0.01 to 3.00 mm were found in similar proportions, and fragments and PE overwhelmed (more than 70 % each). Additionally, AP concentration at S3 was among the highest compared to the whole studied area, and MP concentration was the highest (0.20 MP.m^{-3}). This singular pattern is likely related to the hydrodynamics and the key role of the channels in regulating the exchange of water and matter between the lagoon and the surrounding environment. This region is characterized by high residual fluxes and strong currents mainly generated by tides (up to 2.3 m.s^{-1}, Plus et al., 2009). As water flows in and out of the lagoon through the channels, it may bring in particles from the surrounding land and sea. In addition, fronts are a common feature of these systems (Valle-Levinson, 2022). They are suspected to influence the dispersion pathway of plastic particles as well as their accumulation and trapping (Suaria et al., 2021). Indeed, fronts can create a physical barrier that prevents the mixing of water bodies and form convergence flows that accumulate suspended matter and contaminants such as AP and MP (Suaria et al., 2021; Wang et al., 2022). All these processes could lead to preferential transport pathways of AP and MP at the inlet station in sea surface samples. This phenomenon will be the object of future numerical studies of particle transport in the bay to target preferential transport pathways, or « microplastic *crossroad* » as proposed by Baudena et al. (2022).

The stations located in the middle and the back of the bay (S4 and S5) were characterized by the predominance of fiber-shaped particles (at least 55 %). Moreover, AP and MP concentrations were almost systematically lower than at the other stations (down to 0.02 MP.m^{-3}). The reduced sinking rate of fiber-shaped particles (Bagaev et al., 2017; Jalón-Rojas et al., 2022) may favor their horizontal distribution, vertical mixing and presence at the surface layer. Additionally, the back of the bay is drained off during ebb and samplings were made at low tide and reversal time. Thus, ebb currents may have favored the dispersion of buoyant fragments toward the lagoon inlet. Moreover, ebb currents and repeated water flushing may have limited the transport and accumulation of AP and MP in this area. Finally, the water flow is calmer than at other stations (IFREMER, 2007). Almost 46 Km^2 of the area is covered by *Zostera noltii* seagrass meadows (Plus et al., 2010), influencing the hydrodynamics of the area with a tendency of reducing the water flow (Ganthy et al., 2015; Kombiadou et al., 2014). These conditions may have favored the trapping of suspended particles such as fibers.

On another note, more than half of unknown polymers from S5 were similar white fragments with the same unidentified spectral fingerprint. The matching can have failed due to the absence of the polymer type in libraries (environmental, industrial and online ones). Moreover, some spectra displayed extra or less IR peaks compared to referenced spectra in libraries. These differences can be due to manufacturing (addition of additives) or weathering processes (De Frond et al., 2021; ter Halle et al., 2017). Other unknown spectra can be due to the formation of a biofilm (McGivney et al., 2020) or to their insufficient quality (e.g. weak absorbance and no peaks recorded) when particles are too small or too thin for instance.

4.2. Water column

In the water column, mean AP and MP concentrations were between 1.5 and 8 times higher at outside stations (S1 and S2) than at inside stations, reaching nearly 2000 AP.m^{-3}. As for surface waters, local input sources of particles such as the wastewater discharge point can partly explain higher AP and MP contamination at outside stations than at inside stations. Additionally, rubbery fragments tended to display higher proportions at outside stations compared to inside stations. These particles were similar in shape and texture to tire particles and may come from the WWTP drainage pipe located close to S2 (see Section 4.1 and associated references). However, a higher concentration of AP was found at S1 than at S2, mainly driven by its higher proportion of rubbery fragments. This result suggests that other factors could influence the profile of contamination at outside stations, such as another source of

contamination (e.g. from maritime activities) or oceanic conditions (e.g. shifting direction of the longshore drift).

At inside stations (S3, S4 and S5), concentrations were relatively lower (down to nearly 340 AP.m^{-3}) and fibers overwhelmed (at least 79 %) in comparison with outside stations. As explained in Section 4.1, the inner bay is cyclically drained-off by tides, so fibers are probably transported in suspension by tidal currents. Some of them may also be deposited due to the lower flow and turbulence (Fig. 4) and resuspended with the next incoming tide. Stating a specific reason that may explain lower concentrations found inside the bay compared to outside stations is difficult, but both the absence of an important input source and the specific hydrodynamics of this area may contribute to this pattern. Future studies based on numerical models will provide insights into this question.

For the most part, PET and CELL polymers along with fibers and rubbery fragments were predominant in the water column. These particles are characterized by very low sinking rates and are easily kept in suspension in the water column by currents and turbulences, which can explain their presence at all stations. On another note, shape and polymer characteristics can provide insights into the origin of the contamination. Fibers made of cellulose, PET, PA and PA/CELL, are likely to come from textile tear and wear (Salvador Cesa et al., 2017). Indeed, the global fiber production was around 110 million tons in 2021, which is almost the double of the production in 2000 (TextileExchange, 2022). This production includes cellulosic fibers such as cotton or viscose and synthetic fibers such as PET and PA (TextileExchange, 2022). Part of these fibers can be released into the environment by WWTP effluents (Conley et al., 2019; Weis et al., 2022). Additionally, fibers can enter the environment by atmospheric fallout and this pathway may emit even more fibers than WWTP, as shown for two coastal cities in the United-Kingdom (Napper et al., 2023). It was also suggested that synthetic fibers can come from the degradation of fishing gears (Xue et al., 2020). Finally, other nonwoven products such as wet wipes or disposable masks can be a source of fibers in the environment (Kwon et al., 2022; Ó'Briain et al., 2020).

4.3. Intertidal sediment and Pacific oyster

In sediment and oyster compartments, no spatial variation was highlighted regarding AP and MP concentrations within these two compartments. Additionally, fibers represented at least 85 % and 82 % of particles in studied stations, respectively in sediment and oyster samples. Cellulose was identified at least at 57 % and 47 %, respectively in sediment and oyster samples. Despite slight environmental variations in sediment characteristics and oyster substrates, the pattern of contamination was homogenous within studied stations. These matrices may reflect a time or space integrative contamination. Indeed, the upper 5 cm layer of intertidal sediments was sampled and thus it represented the buried fraction of AP and MP which accumulated over time. Regarding wild oysters, samples is representative of a time integrative contamination as the contamination can result from the filtration and accumulation of particles over several hours or days prior to the sampling.

4.4. Transport of AP and MP in the Arcachon Bay and potential sources

Despite overlapping in particle length ranges between studied samples, sampling and preparation were not performed using the same cut-off threshold. Sea surface was sampled using a net with a 300 µm mesh size, water column was sampled with a pump flowing on a 50 µm mesh-sized sieve and sediments and oysters consisted of bulk samples. Then, sea surface samples were filtrated on a 100 µm mesh size and other sample types on a 50 µm mesh size. As such, insights on transport dynamics suggested in this section have to be considered carefully and should be tested by future in-depth studies, and we do not claim to depict a complete description of all processes driving AP and MP transport. Nonetheless, based on the multi-compartment approach adopted in this study, we provide a conceptual description of AP and MP horizontal and vertical distributions along with their potential transport patterns and sources in the Arcachon Bay (Fig. 6). Moreover, we provided additional data on shape distribution and concentration of AP with length superior to 300 µm (Supp. Mat. 10 and Supp. Mat. 11, respectively).

At the sea surface, samples were firstly composed of fragments (nearly 50 % of AP above 300 µm, Supp. Mat. 10) and PE (almost 48 %) which is a polymer considered as buoyant as it has a density inferior to seawater (Chubarenko et al., 2018; Kooi et al., 2016; Morét-Ferguson et al., 2010). On the contrary, in all other sample types, fragments represented less than 7 % and PE less than 9 %. Hence, it suggests that buoyant fragments tend to accumulate preferentially at the sea surface and there is a limited transport to the water column, intertidal sediments

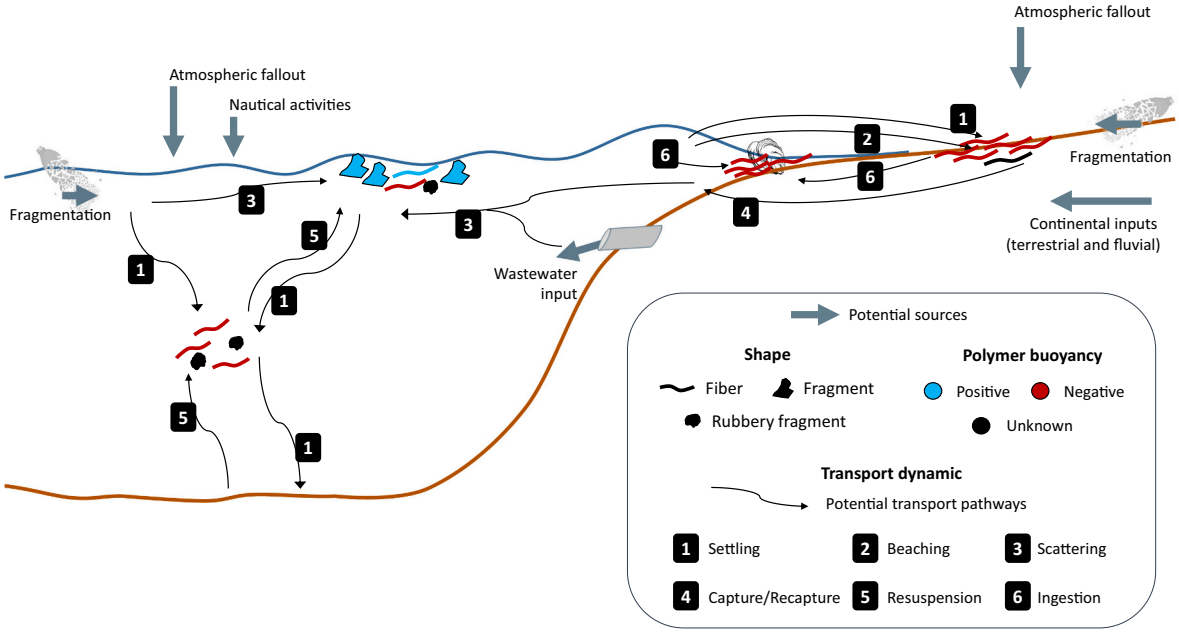

Fig. 6. Conceptual diagram of overall AP and MP contamination in the different compartments, potential transport pathways and sources the in Arcachon Bay.

and oysters (Fig. 6). In parallel, fibers seem to show a great dispersal ability across marine compartments. They were present at the sea surface (nearly 36 % of AP above 300 μm), in the water column (nearly 92 % of AP above 300 μm, otherwise 56 %) and particularly in sediments and oysters (at least 92 % of AP above 300 μm, Supp. Mat. 10). Indeed, they have a lower settling velocity (Jalón-Rojas et al., 2022) and higher sensitivity to small turbulences compared to fragments for instance (Ballent et al., 2012). The polymer density also certainly influences the dispersion of particles. Actually, CELL and PET were mainly identified in the water column (respectively around 40 % and 20 %) and CELL was the main polymer identified in sediment and oyster samples (at least 56 %). These polymers tend to sink as they have a density superior to seawater (Chubarenko et al., 2018). Thus, they can settle more easily than lighter polymers like PE and PP (Kooi et al., 2017). Additionally, the reduced fraction of low-density particles found in other samples than sea surface ones tends to suggest that biofouling barely promotes the sinking of buoyant particles in this system as already described in Jalón-Rojas et al. (2022). This may be partly related to the quick water renewal of the bay (lower than 20 days, Plus et al., 2009). Finally, these results are consistent with a meta-analysis from Erni-Cassola et al. (2019) reporting high proportions of denser polymers in deeper compartments.

Interestingly, no industrial pellets were found in the studied compartments while they were previously recorded in important proportions in the high tide line of sandy beaches from the Arcachon Bay (Lefebvre et al., 2021). In two Brazilian bays, pellets were also found in the high tide line of beaches but not at the sea surface nor in bottom sediment samples (Castro et al., 2020). A hypothesis may be that this type of particle remains close to the coastline by onshore transport mechanisms and beaches easily. However, their total absence remains intriguing, particularly at the sea surface.

Regarding the overall transport dynamic, multiple processes are likely to affect the transport of particles in the Arcachon Bay (Fig. 6). AP and MP in intertidal sediments can come from the settling of particles from the water column, in particular small, mobile and dense ones such as negatively buoyant fibers (Fig. 6). Particles could also beach and end up in intertidal sediments but can also be captured by tides and end up in seawater (Fig. 6). Once in seawater, they can be transported and scattered by currents, waves and wind for instance (e.g. Isobe et al., 2014; Li et al., 2020). On one hand, negatively buoyant particles could partly settle to the water column while buoyant ones are likely staying at the sea surface (Fig. 6). On another hand, AP and MP could oscillate in the water column and even resurface (Kooi et al., 2017) or could be resuspended from intertidal sediment to the water column (Shamskhany et al., 2021). Regarding oysters, their habitat is associated with the sediment compartment and the water column as it is a benthic species and a filter feeder that feed upon suspended particles in the water column. Here, the main shape and polymer type in oyster were also the main ones found in sediment and water column samples in corresponding stations (S3 to S5). Thus, oysters may have ingested AP from water column and/or resuspended AP from intertidal sediments (Fig. 6).

Several sources of AP and MP can be suspected for the Arcachon Bay (Fig. 6). The wastewater drainage pipe located at S2 can represents an important direct input of AP and MP as already shown in other studies (Kazour et al., 2019b). In situ fragmentation upon weathering processes in water or sediment compartment can also be considered as a source of AP and MP. Indeed, beach litter monitoring was conducted in the frame of the MSFD in April 2019 (Lacroix et al., 2022). Besides unidentified fragments, the majority of macroplastics (> 2.5 cm) at beaches close to S1 and S2 (< 2 km) were sections of fishing nets and food packagings, known to be mainly made of PE (Cedre, 2021). Macroplastic monitoring at the back of the bay (Le Teich beach) highlighted a majority of fragmented oyster bags and entire spat collector mainly composed of PE and PP, respectively (Cedre, 2021). The fragmentation of these PE and PP macroplastics could be a direct source of MP. Furthermore, nautical activities among which the above-mentioned fishing and aquaculture sectors can be a source of MP (Lusher et al., 2017; Xue et al., 2020). Additionally, AP and MP can come from freshwater discharges (e.g. Meijer et al., 2021), such as the Leyre River (first freshwater contributor of Arcachon Bay) which is crossing many agricultural lands and historical landfills. Finally, atmospheric fallouts (e.g. Dris et al., 2016) and continental inputs (e.g. UNEP, 2021) have also to be considered as potential sources of AP and MP.

This field study tends to confirm that polymers and morphometric characteristics play a role in particles behavior and distribution, as previously reported in experimental studies (e.g. Bagaev et al., 2017; Enders et al., 2015; Forsberg et al., 2020; Jalón-Rojas et al., 2022). Yet, define horizontal and vertical motions of such a diverse range of particles is still challenging. Numerical simulations at a high spatial resolution are needed in order to evaluate and understands variations at the local scale, especially when the studied area has a complex dynamic. Hence, futures studies will attempt to better understand the transport of MP and AP in the Arcachon Bay by the use of a 3D-model developed for the transport of MP (Jalón-Rojas et al., 2019b) combined with a hydrodynamic model of the area (Lazure and Dumas, 2008).

4.5. Comparisons

Comparisons with other studies must be taken carefully as definitions for AP and MP, sampling methods, analyses and unit reporting are not standardized. Concentrations of AP or MP were compared with the most suitable studies available by checking different criteria including the studied area (coastal zone preferred), size range of particles and polymer identification (preferred). Moreover, except one study which excluded fibers for MP calculation (Frère et al., 2017), other studies cited below included fibers in their analysis.

Here, the mean AP concentration at sea surface (0.15 ± 0.10 AP.m^{-3}) was comparable to the one found in Todos Santos Bay in Mexico (0.19 ± 0.21 items.m^{-3}, Ramírez-Álvarez et al., 2020). However, AP concentration was lower than in the Galway Bay (0.56 ± 0.33 items.m^{-3}, Frias et al., 2020). The mean MP concentration in the present study (0.10 ± 0.08 MP.m^{-3}) was in the same order of magnitude than in the bay of Brest located in the Atlantic coast of France (0.13 ± 0.13 MP.m^{-3}) although fibers were excluded from MP calculation (Frère et al., 2017). In the water column, AP concentrations ranged from 13 to 501 AP.m^{-3} in the North Atlantic Subtropical Gyre (Enders et al., 2015) while the mean concentration was 2080 ± 2190 items.m^{-3} in the Northeast Pacific Ocean (Desforges et al., 2014). Compared to these studies, AP concentration was intermediate in the Arcachon Bay (952.4 ± 661.3 AP.m^{-3}). Here, the cut-off threshold do not seems to explain much of the difference described for water column and sea surface samples (respectively filtrated on 50 μm and 100 μm mesh size in this study). Indeed, higher concentrations were found in studies displaying similar cut off threshold (filtration on 62 μm for water column samples in Desforges et al., 2014 and 100 μm for sea surface samples by Frias et al., 2020). Lower concentrations were described while using a lower cut-off threshold (10 μm mesh size in Enders et al., 2015). Finally, similar concentrations can be described by using a higher cut off threshold (AP above 250 μm considered in sea surface samples from Ramírez-Álvarez et al., 2020) or lower mesh size for samples filtration (1.6 μm in Frère et al., 2017). Hence, differences between studies for AP mean concentrations in seawater may be inherent to the studied area (e.g. hydrodynamics, intensity and type of anthropic pressures or distance from input sources).

In intertidal sediments, AP and MP mean concentrations were clearly lower in this study (40.10 ± 33.40 AP.kg^{-1} dw) than the ones reported in sandy beaches from the North of France (around 150 items.kg^{-1} dw, Lots et al., 2017) and across the Atlantic Ocean (238 items.kg^{-1} dw, Lots et al., 2017). Even though the difference was less marked, AP mean concentration was also lower than the reported one from beaches in Belgium (92.0 ± 25.6 items.kg^{-1} dw, Claessens et al., 2011). Additionally, mean MP concentration from this study (6.91 ± 9.25 MP.kg^{-1} dw) was also clearly lower than the ones recorded in sandy beaches from

the Atlantic coast of France where concentrations reached 457.1 MP. kg^{-1} (Bringer et al., 2021). Different cut-off thresholds can explain these differences as higher discrepancies tend to be associated with lower cut-of thresholds (filtration on 50 μm in this study, on 38 μm in Claessens et al., 2011, on 0.45 μm in Lots et al., 2017 and on 0.2 μm in Bringer et al., 2021). Moreover, local environmental conditions and anthropogenic pressures can influence MP concentrations in sediments (e.g. Browne et al., 2011; Jorquera et al., 2022), which can partly explain these differences too.

Regarding oyster contamination, AP mean concentration from the Arcachon Bay was 0.33 ± 0.50 AP.g^{-1} fw (or 2.42 ± 2.50 AP.ind^{-1}) and MP mean concentration was 0.13 ± 0.26 MP.g^{-1} fw (or 0.94 ± 1.56 MP. ind^{-1}). AP concentrations in tissues of oysters from the lagoon of Bizerte tended to be higher than at the Arcachon Bay (1.48 items.g^{-1}, Abidli et al., 2019). Moreover, MP concentrations in oysters from the Atlantic coast of France tended to be slightly higher (0.23 ± 0.20 MP.g^{-1} fw, Phuong et al., 2018b) than in the Arcachon Bay, and abundances per individual were almost two times higher (2.1 ± 1.7 MP.ind^{-1}; Phuong et al., 2018b). These disparities could be explained by the cut-off threshold used in studies (50 μm in this study; 12 μm in Phuong et al., 2018b; 1 μm in Abidli et al., 2019). As for other type of sample, environmental processes or anthropic pressures (level and types) are different across locations and it can greatly influence the contamination level of the area and the uptake of AP and MP by oysters.

5. Conclusion

AP and MP distribution at the sea surface and in the water column of the Arcachon Bay displayed spatial variabilities (quantitatively and qualitatively). Three contamination patterns were described at the sea surface (outside stations, inlet station, inner stations) while two patterns were described in the water column (outside stations and inside stations). These profiles were probably influenced by the complex hydrodynamics of the Arcachon Bay and the proximity of an input source of particles (wastewater drainage pipe). On the contrary, sediment and oyster samples showed homogenous contamination profiles between studied stations. Overall, buoyant fragments were rather found at the sea surface while fibers and negatively buoyant particles were rather detected in water column, intertidal sediments and oyster samples. This supports the hypothesis that morphometric and chemical characteristics can influence the vertical distribution of AP and MP between marine compartments. Additionally, the prevalence of cellulosic fibers highlights the importance of this type of contamination in marine ecosystems. Moreover, it suggests that part of the contamination could be due to textile tear and wear. These findings underline the importance of considering a wide range of AP in order to provide accurate estimations of the contamination and determine sources. Finally, AP and MP were recorded at all stations from all the studied compartments, attesting to their already known ubiquity in marine ecosystems.

Funding

This study was conducted in the frame of the ARPLASTIC regional research project. This project was funded by the *Nouvelle-Aquitaine* region, the *Agence de l'Eau Adour-Garonne*, the *Syndicat Intercommunal du Bassin d'Arcachon* (SIBA) and the *Parc National Marin du Bassin d'Arcachon - Office Français de la Biodiversité* (PNMBA - OFB). The French Minister of Higher Education, Research & Innovation, provided additional funding for Charlotte Lefebvre's PhD grant.

CRediT authorship contribution statement

This study was conceptualized by FLB, BM, SL, CL and JC. BM, FLB, JC and SL acquired the financial support and BM managed the project. Methodologies were set up by BM, CC, CL, FLB, JC and SL. Samplings were made by FLB and CL. Sample preparation and analysis were made by CL, FLB, CC, ED, JB and LCV. Data harmonization, data visualization and statistical analysis were made by CL. Resources were provided by BM, CC, JC, and SL. CL wrote the original draft and BM, FLB, IJR, SL, and JC reviewed the manuscript. JC, SL and BM supervised CL. FLB, CL and JC supervised ED and LCV. CL and SL supervised JB. All authors contributed to the article and approved the submitted version.

Declaration of competing interest

The authors declare that they have no known competing financial interests or personal relationships that could have appeared to influence the work reported in this paper.

Data availability

Data will be made available on request.

Acknowledgments

This study was conducted within the frame of the JPI Oceans Response project. Samplings were made thanks to marine facilities provided by the SIBA and the PNMBA. Authors would like to give special thanks to the captains and crews who made samplings possible: Denis Dubos, Jean-Philippe Besse and Mohamed Benyahia from the SIBA and Romuald Chaigneau, Olivier Trevidic and Virginie Rog from the PNMBA. Moreover, we would like to thanks Jean Latrille and Melissa Tanfin for the preliminary analysis of sea surface samples and the setup of protocol extraction in sediment samples. Finally, authors would like to thanks Georges Lacaze for its involvement in the construction of the homemade filtration system.

Appendix A. Supplementary data

Supplementary data to this article can be found online at https://doi.org/10.1016/j.scitotenv.2023.165460.

References

Abidli, S., Lahbib, Y., Trigui El Menif, N., 2019. Microplastics in commercial molluscs from the lagoon of Bizerte (northern Tunisia). Mar. Pollut. Bull. 142, 243–252. https://doi.org/10.1016/j.marpolbul.2019.03.048.

Adams, J.K., Dean, B.Y., Athey, S.N., Jantunen, L.M., Bernstein, S., Stern, G., Diamond, M.L., Finkelstein, S.A., 2021. Anthropogenic particles (including microfibers and microplastics) in marine sediments of the Canadian Arctic. Sci. Total Environ. 784, 147155 https://doi.org/10.1016/j.scitotenv.2021.147155.

Andrady, A.L., 2011. Microplastics in the marine environment. Mar. Pollut. Bull. 62, 1596–1605. https://doi.org/10.1016/j.marpolbul.2011.05.030.

Arias, A.H., Alfonso, M.B., Girones, L., Piccolo, M.C., Marcovecchio, J.E., 2022. Synthetic microfibers and tyre wear particles pollution in aquatic systems: relevance and mitigation strategies. Environ. Pollut. 295, 118607 https://doi.org/10.1016/j.envpol.2021.118607.

Auguie, B., Antonov, A., 2017. gridExtra: Miscellaneous Functions for "Grid" Graphics. R Package Version 2.

Bagaev, A., Mizyuk, A., Khatmullina, L., Isachenko, I., Chubarenko, I., 2017. Anthropogenic fibres in the Baltic Sea water column: field data, laboratory and numerical testing of their motion. Sci. Total Environ. 599–600, 560–571. https://doi.org/10.1016/j.scitotenv.2017.04.185.

Ballent, A., Purser, A., de Jesus Mendes, P., Pando, S., Thomsen, L., 2012. Physical transport properties of marine microplastic pollution (preprint). In: Biodiversity and Ecosystem Function: Marine. https://doi.org/10.5194/bgd-9-18755-2012.

Balthazar-Silva, D., Turra, A., Moreira, F.T., Camargo, R.M., Oliveira, A.L., Barbosa, L., Gorman, D., 2020. Rainfall and tidal cycle regulate seasonal inputs of microplastic pellets to sandy beaches. Front. Environ. Sci. 8, 123. https://doi.org/10.3389/fenvs.2020.00123.

Barnes, D.K.A., 2005. Remote Islands reveal rapid rise of southern hemisphere sea debris. Sci. World J. 5, 915–921. https://doi.org/10.1100/tsw.2005.120.

Baudena, A., Ser-Giacomi, E., Jalón-Rojas, I., Galgani, F., Pedrotti, M.L., 2022. The streaming of plastic in the Mediterranean Sea. Nat. Commun. 13, 2981. https://doi.org/10.1038/s41467-022-30572-5.

Bergmann, M., Gutow, L., Klages, M., Alfred-Wegener-Institut, Göteborgs universitet (Eds.), 2015. Marine Anthropogenic Litter, Springer Open. Springer, Cham Heidelberg New York Dordrecht London.

Blanchet, H., de Montaudouin, X., Chardy, P., Bachelet, G., 2005. Structuring factors and recent changes in subtidal macrozoobenthic communities of a coastal lagoon,

Arcachon Bay (France). Estuar. Coast. Shelf Sci. 64, 561–576. https://doi.org/10.1016/j.ecss.2005.03.016.
Boucher, J., Friot, D., 2017. Primary microplastics in the oceans: a global evaluation of sources. In: IUCN International Union for Conservation of Nature.. https://doi.org/10.2305/IUCN.CH.2017.01.en.
Bråte, I.L.N., Hurley, R., Lusher, A., Buenaventura, N., Hultman, M., Halsband, C., Green, N., 2020. Microplastics in Marine Bivalves from the Nordic Environment. Nordic Council of Ministers.
Bringer, A., Le Floch, S., Kerstan, A., Thomas, H., 2021. Coastal ecosystem inventory with characterization and identification of plastic contamination and additives from aquaculture materials. Mar. Pollut. Bull. 167, 112286 https://doi.org/10.1016/j.marpolbul.2021.112286.
Browne, M.A., Crump, P., Niven, S.J., Teuten, E., Tonkin, A., Galloway, T., Thompson, R., 2011. Accumulation of microplastic on shorelines woldwide: sources and sinks. Environ. Sci. Technol. 45, 9175–9179. https://doi.org/10.1021/es201811s.
Bucci, K., Rochman, C.M., 2022. Microplastics: a multidimensional contaminant requires a multidimensional framework for assessing risk. Microplastics Nanoplastics 2, 7. https://doi.org/10.1186/s43591-022-00028-0.
Carlsson, P., Singdahl-Larsen, C., Lusher, A.L., 2021. Understanding the occurrence and fate of microplastics in coastal Arctic ecosystems: the case of surface waters, sediments and walrus (Odobenus rosmarus). Sci. Total Environ. 792, 148308 https://doi.org/10.1016/j.scitotenv.2021.148308.
Castel, J., Labourg, P.-J., Escaravage, V., Auby, I., Garcia, M.E., 1989. Influence of seagrass beds and oyster parks on the abundance and biomass patterns of meio- and macrobenthos in tidal flats. Estuar. Coast. Shelf Sci. 28, 71–85. https://doi.org/10.1016/0272-7714(89)90042-5.
Castelle, B., Bonneton, P., Dupuis, H., Sénéchal, N., 2007. Double bar beach dynamics on the high-energy meso-macrotidal French Aquitanian coast: a review. Mar. Geol. 245, 141–159. https://doi.org/10.1016/j.margeo.2007.06.001.
Castro, R.O., da Silva, M.L., Marques, M.R.C., de Araújo, F.V., 2020. Spatio-temporal evaluation of macro, meso and microplastics in surface waters, bottom and beach sediments of two embayments in Niterói, RJ, Brazil. Mar. Pollut. Bull. 160, 111537 https://doi.org/10.1016/j.marpolbul.2020.111537.
Cayocca, F., 2001. Long-term morphological modeling of a tidal inlet: the Arcachon Basin, France. Coast. Eng. 42, 115–142. https://doi.org/10.1016/S0378-3839(00)00053-3.
Cedre, 2021. Réseau national de surveillance des macrodéchets sur le littoral (2015 à 2021). Public data extracted on 09/10/2021 [WWW Document]. URL. https://surval.ifremer.fr/Donnees/Cartographie-Donnees-par-parametre#/map.
Chiba, S., Saito, H., Fletcher, R., Yogi, T., Kayo, M., Miyagi, S., Ogido, M., Fujikura, K., 2018. Human footprint in the abyss: 30 year records of deep-sea plastic debris. Mar. Policy 96, 204–212. https://doi.org/10.1016/j.marpol.2018.03.022.
Chubarenko, I., Esiukova, E., Bagaev, A., Isachenko, I., Demchenko, N., Zobkov, M., Efimova, I., Bagaeva, M., Khatmullina, L., 2018. Behavior of microplastics in coastal zones. In: Microplastic Contamination in Aquatic Environments. Elsevier, pp. 175–223.
Claessens, M., Meester, S.D., Landuyt, L.V., Clerck, K.D., Janssen, C.R., 2011. Occurrence and distribution of microplastics in marine sediments along the Belgian coast. Mar. Pollut. Bull. 62, 2199–2204. https://doi.org/10.1016/j.marpolbul.2011.06.030.
Cole, M., Lindeque, P., Halsband, C., Galloway, T.S., 2011. Microplastics as contaminants in the marine environment: a review. Mar. Pollut. Bull. 62, 2588–2597. https://doi.org/10.1016/j.marpolbul.2011.09.025.
Collard, F., Gasperi, J., Gilbert, B., Eppe, G., Azimi, S., Rocher, V., Tassin, B., 2018. Anthropogenic particles in the stomach contents and liver of the freshwater fish Squalius cephalus. Sci. Total Environ. 643, 1257–1264. https://doi.org/10.1016/j.scitotenv.2018.06.313.
Conley, K., Clum, A., Deepe, J., Lane, H., Beckingham, B., 2019. Wastewater treatment plants as a source of microplastics to an urban estuary: removal efficiencies and loading per capita over one year. Water Res. X 3, 100030. https://doi.org/10.1016/j.wroa.2019.100030.
Courtene-Jones, W., Maddalene, T., James, M.K., Smith, N.S., Youngblood, K., Jambeck, J.R., Earthrowl, S., Delvalle-Borrero, D., Penn, E., Thompson, R.C., 2021. Source, sea and sink—a holistic approach to understanding plastic pollution in the southern Caribbean. Sci. Total Environ. 797, 149098 https://doi.org/10.1016/j.scitotenv.2021.149098.
Crichton, E.M., Noël, M., Gies, E.A., Ross, P.S., 2017. A novel, density-independent and FTIR-compatible approach for the rapid extraction of microplastics from aquatic sediments. Anal. Methods 9, 1419–1428. https://doi.org/10.1039/C6AY02733D.
De Frond, H., Rubinovitz, R., Rochman, C.M., 2021. μATR-FTIR spectral libraries of plastic particles (FLOPP and FLOPP-e) for the analysis of microplastics. Anal. Chem. 93, 15878–15885.
Dehaut, A., Cassone, A.-L., Frère, L., Hermabessiere, L., Himber, C., Rinnert, E., Rivière, G., Lambert, C., Soudant, P., Huvet, A., Duflos, G., Paul-Pont, I., 2016. Microplastics in seafood: benchmark protocol for their extraction and characterization. Environ. Pollut. 215, 223–233. https://doi.org/10.1016/j.envpol.2016.05.018.
Desforges, J.-P.W., Galbraith, M., Dangerfield, N., Ross, P.S., 2014. Widespread distribution of microplastics in subsurface seawater in the NE Pacific Ocean. Mar. Pollut. Bull. 79, 94–99. https://doi.org/10.1016/j.marpolbul.2013.12.035.
Desforges, J.-P.W., Galbraith, M., Ross, P.S., 2015. Ingestion of microplastics by zooplankton in the Northeast Pacific Ocean. Arch. Environ. Contam. Toxicol. 69, 320–330. https://doi.org/10.1007/s00244-015-0172-5.
Dris, R., Gasperi, J., Saad, M., Mirande, C., Tassin, B., 2016. Synthetic fibers in atmospheric fallout: a source of microplastics in the environment? Mar. Pollut. Bull. 104, 290–293. https://doi.org/10.1016/j.marpolbul.2016.01.006.
Eisentraut, P., Dümichen, E., Ruhl, A.S., Jekel, M., Albrecht, M., Gehde, M., Braun, U., 2018. Two birds with one stone—fast and simultaneous analysis of microplastics: microparticles derived from thermoplastics and tire wear. Environ. Sci. Technol. Lett. 5, 608–613. https://doi.org/10.1021/acs.estlett.8b00446.
Enders, K., Lenz, R., Stedmon, C.A., Nielsen, T.G., 2015. Abundance, size and polymer composition of marine microplastics ≥ 10 μm in the Atlantic Ocean and their modelled vertical distribution. Mar. Pollut. Bull. 100, 70–81. https://doi.org/10.1016/j.marpolbul.2015.09.027.
Erni-Cassola, G., Zadjelovic, V., Gibson, M.I., Christie-Oleza, J.A., 2019. Distribution of plastic polymer types in the marine environment; a meta-analysis. J. Hazard. Mater. 369, 691–698. https://doi.org/10.1016/j.jhazmat.2019.02.067.
Firke, S., 2021. Janitor: Simple Tools for Examining and Cleaning Dirty Data (2020). R Package Version 2.1.0.
Forsberg, P.L., Sous, D., Stocchino, A., Chemin, R., 2020. Behaviour of plastic litter in nearshore waters: first insights from wind and wave laboratory experiments. Mar. Pollut. Bull. 153, 111023 https://doi.org/10.1016/j.marpolbul.2020.111023.
Fox, J., Weisberg, S., 2018. An R Companion to Applied Regression.
Frère, L., Paul-Pont, I., Rinnert, E., Petton, S., Jaffré, J., Bihannic, I., Soudant, P., Lambert, C., Huvet, A., 2017. Influence of environmental and anthropogenic factors on the composition, concentration and spatial distribution of microplastics: a case study of the Bay of Brest (Brittany, France). Environ. Pollut. 225, 211–222. https://doi.org/10.1016/j.envpol.2017.03.023.
Frias, J.P.G.L., Nash, R., 2019. Microplastics: finding a consensus on the definition. Mar. Pollut. Bull. 138, 145–147. https://doi.org/10.1016/j.marpolbul.2018.11.022.
Frias, J.P.G.L., Lyashevska, O., Joyce, H., Pagter, E., Nash, R., 2020. Floating microplastics in a coastal embayment: a multifaceted issue. Mar. Pollut. Bull. 158, 111361 https://doi.org/10.1016/j.marpolbul.2020.111361.
Ganthy, F., Soissons, L., Sauriau, P.-G., Verney, R., Sottolichio, A., 2015. Effects of short flexible seagrass *Zostera noltei* on flow, erosion and deposition processes determined using flume experiments. Sedimentology 62, 997–1023. https://doi.org/10.1111/sed.12170.
GESAMP, 2015. Sources, fate and effects of microplastics in the marine environment: a global assessment. In: Rep. Stud. GESAMP No. 90. IMO/FAO/UNESCO-IOC/UNIDO/WMO/IAEA/UN/UNEP/UNDP Joint Group of Experts on the Scientific Aspects of Marine Environmental Protection.
GESAMP, 2019. Guidelines for the Monitoring and Assessment of Plastic Litter and Microplastics in the Ocean.
Geyer, R., Jambeck, J.R., Law, K.L., 2017. Production, use, and fate of all plastics ever made. Sci. Adv. 3, e1700782 https://doi.org/10.1126/sciadv.1700782.
Goverse, T., United Nations, Environment Programme, Division of Early Warning and Assessment, 2014. UNEP Year Book 2014 Emerging Issues in our Global Environment. United Nations Environment Programme (UNEP), Nairobi.
Gündoğdu, S., Ayat, B., Aydoğan, B., Çevik, C., Karaca, S., 2022. Hydrometeorological assessments of the transport of microplastic pellets in the eastern Mediterranean. Sci. Total Environ. 823, 153676 https://doi.org/10.1016/j.scitotenv.2022.153676.
Hidalgo-Ruz, V., Gutow, L., Thompson, R.C., Thiel, M., 2012. Microplastics in the marine environment: a review of the methods used for identification and quantification. Environ. Sci. Technol. 46, 3060–3075. https://doi.org/10.1021/es2031505.
Huntington, A., Corcoran, P.L., Jantunen, L., Thaysen, C., Bernstein, S., Stern, G.A., Rochman, C.M., 2020. A first assessment of microplastics and other anthropogenic particles in Hudson Bay and the surrounding eastern Canadian Arctic waters of Nunavut. FACETS 5, 432–454. https://doi.org/10.1139/facets-2019-0042.
Idier, D., Castelle, B., Charles, E., Mallet, C., 2013. Longshore sediment flux hindcast: spatio-temporal variability along the SW Atlantic coast of France. J. Coast. Res. 1785–1790.
IFREMER, 2007. Caractérisation des composantes hydrodynamiques d'une lagune mésotidale, le Bassin d'Arcachon, p. 54.
Imhof, H.K., Sigl, R., Brauer, E., Feyl, S., Giesemann, P., Klink, S., Leupolz, K., Löder, M.G.J., Löschel, L.A., Missun, J., Muszynski, S., Ramsperger, A.F.R.M., Schrank, I., Speck, S., Steibl, S., Trotter, B., Winter, I., Laforsch, C., 2017. Spatial and temporal variation of macro-, meso- and microplastic abundance on a remote coral island of the Maldives, Indian Ocean. Mar. Pollut. Bull. 116, 340–347. https://doi.org/10.1016/j.marpolbul.2017.01.010.
Institut national de la statistique et des études économiques, 2023. https://www.insee.fr/fr/statistiques/2011101?geo=ARR-336#chiffre-cle-1. (Accessed 27 February 2023).
Isobe, A., Kubo, K., Tamura, Y., Kako, S., Nakashima, E., Fujii, N., 2014. Selective transport of microplastics and mesoplastics by drifting in coastal waters. Mar. Pollut. Bull. 89, 324–330. https://doi.org/10.1016/j.marpolbul.2014.09.041.
Isobe, A., Iwasaki, S., Uchida, K., Tokai, T., 2019. Abundance of non-conservative microplastics in the upper ocean from 1957 to 2066. Nat. Commun. 10, 417. https://doi.org/10.1038/s41467-019-08316-9.
Jalón-Rojas, I., Wang, X.-H., Fredj, E., 2019a. Technical note: on the importance of a three-dimensional approach for modelling the transport of neustic microplastics. Ocean Sci. 15, 717–724. https://doi.org/10.5194/os-15-717-2019.
Jalón-Rojas, I., Wang, X.H., Fredj, E., 2019b. A 3D numerical model to Track Marine Plastic Debris (TrackMPD): sensitivity of microplastic trajectories and fates to particle dynamical properties and physical processes. Mar. Pollut. Bull. 141, 256–272. https://doi.org/10.1016/j.marpolbul.2019.02.052.
Jalón-Rojas, I., Romero-Ramírez, A., Fauquembergue, K., Rossignol, L., Cachot, J., Sous, D., Morin, B., 2022. Effects of biofilms and particle physical properties on the rising and settling velocities of microplastic fibers and sheets. Environ. Sci. Technol. 56, 8114–8123. https://doi.org/10.1021/acs.est.2c01302.
Jorquera, A., Castillo, C., Murillo, V., Araya, J., Pinochet, J., Narváez, D., Pantoja-Gutiérrez, S., Urbina, M.A., 2022. Physical and anthropogenic drivers shaping the

spatial distribution of microplastics in the marine sediments of Chilean fjords. Sci. Total Environ. 814, 152506 https://doi.org/10.1016/j.scitotenv.2021.152506.
Kaandorp, M.L.A., Dijkstra, H.A., van Sebille, E., 2021. Modelling size distributions of marine plastics under the influence of continuous cascading fragmentation. Environ. Res. Lett. 16, 054075 https://doi.org/10.1088/1748-9326/abe9ea.
Kanhai, L.D.K., Officer, R., Lyashevska, O., Thompson, R.C., O'Connor, I., 2017. Microplastic abundance, distribution and composition along a latitudinal gradient in the Atlantic Ocean. Mar. Pollut. Bull. 115, 307–314. https://doi.org/10.1016/j.marpolbul.2016.12.025.
Kanhai, L.D.K., Gardfeldt, K., Krumpen, T., Thompson, R.C., O'Connor, I., 2020. Microplastics in sea ice and seawater beneath ice floes from the Arctic Ocean. Sci. Rep. 10, 5004. https://doi.org/10.1038/s41598-020-61948-6.
Kassambara, A., 2020. ggpubr:"ggplot2" Based Publication Ready Plots.
Kassambara, A., 2021. rstatix: Pipe-friendly Framework for Basic Statistical Tests (R Package Version 0.7. 0)[Computer Software].
Kazour, M., Jemaa, S., Issa, C., Khalaf, G., Amara, R., 2019a. Microplastics pollution along the Lebanese coast (eastern Mediterranean Basin): occurrence in surface water, sediments and biota samples. Sci. Total Environ. 696, 133933 https://doi.org/10.1016/j.scitotenv.2019.133933.
Kazour, M., Terki, S., Rabhi, K., Jemaa, S., Khalaf, G., Amara, R., 2019b. Sources of microplastics pollution in the marine environment: importance of wastewater treatment plant and coastal landfill. Mar. Pollut. Bull. 146, 608–618. https://doi.org/10.1016/j.marpolbul.2019.06.066.
Kedzierski, M., Villain, J., Falcou-Préfol, M., Kerros, M.E., Henry, M., Pedrotti, M.L., Bruzaud, S., 2019. Microplastics in Mediterranean Sea: a protocol to robustly assess contamination characteristics. PLoS One 14, e0212088. https://doi.org/10.1371/journal.pone.0212088.
Kelly, A., Lannuzel, D., Rodemann, T., Meiners, K.M., Auman, H.J., 2020. Microplastic contamination in East Antarctic Sea ice. Mar. Pollut. Bull. 154, 111130 https://doi.org/10.1016/j.marpolbul.2020.111130.
Klasios, N., De Frond, H., Miller, E., Sedlak, M., Rochman, C.M., 2021. Microplastics and other anthropogenic particles are prevalent in mussels from San Francisco Bay, and show no correlation with PAHs. Environ. Pollut. 271, 116260 https://doi.org/10.1016/j.envpol.2020.116260.
Kole, P.J., Löhr, A.J., Van Belleghem, F., Ragas, A., 2017. Wear and tear of tyres: a stealthy source of microplastics in the environment. Int. J. Environ. Res. Public Health 14, 1265. https://doi.org/10.3390/ijerph14101265.
Kombiadou, K., Ganthy, F., Verney, R., Plus, M., Sottolichio, A., 2014. Modelling the effects of Zostera noltei meadows on sediment dynamics: application to the Arcachon lagoon. Ocean Dyn. 64, 1499–1516. https://doi.org/10.1007/s10236-014-0754-1.
Kooi, M., Reisser, J., Slat, B., Ferrari, F.F., Schmid, M.S., Cunsolo, S., Brambini, R., Noble, K., Sirks, L.-A., Linders, T.E.W., Schoeneich-Argent, R.I., Koelmans, A.A., 2016. The effect of particle properties on the depth profile of buoyant plastics in the ocean. Sci. Rep. 6, 33882. https://doi.org/10.1038/srep33882.
Kooi, M., van Nes, E.H., Scheffer, M., Koelmans, A.A., 2017. Ups and downs in the ocean: effects of biofouling on vertical transport of microplastics. Environ. Sci. Technol. 51, 7963–7971. https://doi.org/10.1021/acs.est.6b04702.
Kwon, S., Zambrano, M.C., Venditti, R.A., Frazier, R., Zambrano, F., Gonzalez, R.W., Pawlak, J.J., 2022. Microfiber shedding from nonwoven materials including wipes and meltblown nonwovens in air and water environments. Environ. Sci. Pollut. Res. 29, 60584–60599. https://doi.org/10.1007/s11356-022-20053-z.
Lacroix, C., André, S., van Loon, W., 2022. Abundance, composition and trends of beach litter. In: OSPAR, 2023: The 2023 Quality Status Report for the North-East Atlantic. OSPAR Commission, London. Available at: https://oap.ospar.org/en/ospar-assessments/quality-status-reports/qsr-2023/indicator-assessments/beach-litter/. Available at:
Lazure, P., Dumas, F., 2008. An external–internal mode coupling for a 3D hydrodynamical model for applications at regional scale (MARS). Adv. Water Resour. 31, 233–250. https://doi.org/10.1016/j.advwatres.2007.06.010.
Leads, R.R., Weinstein, J.E., 2019. Occurrence of tire wear particles and other microplastics within the tributaries of the Charleston Harbor estuary, South Carolina, USA. Mar. Pollut. Bull. 145, 569–582. https://doi.org/10.1016/j.marpolbul.2019.06.061.
Lefebvre, C., Saraux, C., Heitz, O., Nowaczyk, A., Bonnet, D., 2019. Microplastics FTIR characterisation and distribution in the water column and digestive tracts of small pelagic fish in the Gulf of lions. Mar. Pollut. Bull. 142, 510–519. https://doi.org/10.1016/j.marpolbul.2019.03.025.
Lefebvre, C., Rojas, I.J., Lasserre, J., Villette, S., Lecomte, S., Cachot, J., Morin, B., 2021. Stranded in the high tide line: spatial and temporal variability of beached microplastics in a semi-enclosed embayment (Arcachon, France). Sci. Total Environ. 797, 149144 https://doi.org/10.1016/j.scitotenv.2021.149144.
Li, Y., Zhang, H., Tang, C., 2020. A review of possible pathways of marine microplastics transport in the ocean. Anthr. Coasts 3, 6–13. https://doi.org/10.1139/anc-2018-0030.
Lots, F.A.E., Behrens, P., Vijver, M.G., Horton, A.A., Bosker, T., 2017. A large-scale investigation of microplastic contamination: abundance and characteristics of microplastics in European beach sediment. Mar. Pollut. Bull. 123, 219–226. https://doi.org/10.1016/j.marpolbul.2017.08.057.
Lusher, A., Hollman, P., Mendoza-Hill, J., 2017. Microplastics in Fisheries and Aquaculture: Status of Knowledge on Their Occurrence and Implications for Aquatic Organisms and Food Safety. FAO.
MacLeod, M., Arp, H.P.H., Tekman, M.B., Jahnke, A., 2021. The global threat from plastic pollution. Science 373, 61–65. https://doi.org/10.1126/science.abg5433.
Mangiafico, S., 2017. Package 'rcompanion'. In: CRAN Repos, pp. 1–71.
Marine Strategy Framework Directive, 2013. Guidance on Monitoring of Marine Litter in European Seas. Publications Office, LU.
McGivney, E., Cederholm, L., Barth, A., Hakkarainen, M., Hamacher-Barth, E., Ogonowski, M., Gorokhova, E., 2020. Rapid physicochemical changes in microplastic induced by biofilm formation. Front. Bioeng. Biotechnol. 8, 205. https://doi.org/10.3389/fbioe.2020.00205.
Meijer, L.J.J., van Emmerik, T., van der Ent, R., Schmidt, C., Lebreton, L., 2021. More than 1000 rivers account for 80% of global riverine plastic emissions into the ocean. Sci. Adv. 7, eaaz5803 https://doi.org/10.1126/sciadv.aaz5803.
Mishra, A.K., Singh, J., Mishra, P.P., 2021. Microplastics in polar regions: an early warning to the world's pristine ecosystem. Sci. Total Environ. 784, 147149 https://doi.org/10.1016/j.scitotenv.2021.147149.
Mishra, S., Rath, C., Charan, Das, A.P., 2019. Marine microfiber pollution: a review on present status and future challenges. Mar. Pollut. Bull. 140, 188–197. https://doi.org/10.1016/j.marpolbul.2019.01.039.
Moore, C.J., 2008. Synthetic polymers in the marine environment: a rapidly increasing, long-term threat. Environ. Res. 108, 131–139. https://doi.org/10.1016/j.envres.2008.07.025.
Morét-Ferguson, S., Law, K.L., Proskurowski, G., Murphy, E.K., Peacock, E.E., Reddy, C. M., 2010. The size, mass, and composition of plastic debris in the western North Atlantic Ocean. Mar. Pollut. Bull. 60, 1873–1878. https://doi.org/10.1016/j.marpolbul.2010.07.020.
Napper, I.E., Parker-Jurd, F.N.F., Wright, S.L., Thompson, R.C., 2023. Examining the release of synthetic microfibres to the environment via two major pathways: atmospheric deposition and treated wastewater effluent. Sci. Total Environ. 857, 159317 https://doi.org/10.1016/j.scitotenv.2022.159317.
Neuwirth, E., 2014. RColorBrewer: ColorBrewer Palettes. R Package Version 1, pp. 1–2.
Ó'Briain, O., Marques Mendes, A.R., McCarron, S., Healy, M.G., Morrison, L., 2020. The role of wet wipes and sanitary towels as a source of white microplastic fibres in the marine environment. Water Res. 182, 116021 https://doi.org/10.1016/j.watres.2020.116021.
Ogle, D.H., Doll, J.C., Wheeler, P., Dinno, A., 2021. FSA: Fisheries Stock Analysis. R Package Version 0.9, p. 1.
Panti, C., Giannetti, M., Baini, M., Rubegni, F., Minutoli, R., Fossi, M.C., 2015. Occurrence, relative abundance and spatial distribution of microplastics and zooplankton NW of Sardinia in the Pelagos sanctuary protected area, Mediterranean Sea. Environ. Chem. 12, 618. https://doi.org/10.1071/EN14234.
Parker-Jurd, F.N.F., Napper, I.E., Abbott, G.D., Hann, S., Thompson, R.C., 2021. Quantifying the release of tyre wear particles to the marine environment via multiple pathways. Mar. Pollut. Bull. 172, 112897 https://doi.org/10.1016/j.marpolbul.2021.112897.
Phuong, N.N., Poirier, L., Lagarde, F., Kamari, A., Zalouk-Vergnoux, A., 2018a. Microplastic abundance and characteristics in French Atlantic coastal sediments using a new extraction method. Environ. Pollut. 243, 228–237. https://doi.org/10.1016/j.envpol.2018.08.032.
Phuong, N.N., Poirier, L., Pham, Q.T., Lagarde, F., Zalouk-Vergnoux, A., 2018b. Factors influencing the microplastic contamination of bivalves from the French Atlantic coast: location, season and/or mode of life? Mar. Pollut. Bull. 129, 664–674. https://doi.org/10.1016/j.marpolbul.2017.10.054.
Plus, M., Dumas, F., Stanisière, J.-Y., Maurer, D., 2009. Hydrodynamic characterization of the Arcachon Bay, using model-derived descriptors. Cont. Shelf Res. 6.
Plus, M., Dalloyau, S., Trut, G., Auby, I., de Montaudouin, X., Emery, É., Claire, N., Christophe, V., 2010. Long-term evolution (1988–2008) of Zostera spp. meadows in Arcachon Bay (Bay of Biscay). Estuar. Coast. Shelf Sci. 87, 357–366. https://doi.org/10.1016/j.ecss.2010.01.016.
Prata, J.C., Reis, V., Paço, A., Martins, P., Cruz, A., da Costa, J.P., Duarte, A.C., Rocha-Santos, T., 2020. Effects of spatial and seasonal factors on the characteristics and carbonyl index of (micro)plastics in a sandy beach in Aveiro, Portugal. Sci. Total Environ. 709, 135892 https://doi.org/10.1016/j.scitotenv.2019.135892.
Ramírez-Álvarez, N., Rios Mendoza, L.M., Macías-Zamora, J.V., Oregel-Vázquez, L., Alvarez-Aguilar, A., Hernández-Guzmán, F.A., Sánchez-Osorio, J.L., Moore, C.J., Silva-Jiménez, H., Navarro-Olache, L.F., 2020. Microplastics: sources and distribution in surface waters and sediments of Todos Santos Bay, Mexico. Sci. Total Environ. 703, 134838 https://doi.org/10.1016/j.scitotenv.2019.134838.
RStudio Team, 2016. RStudio: Integrated Development Environment for R.
Rudis, B., 2020. Hrbrthemes: additional themes, theme components and utilities for "ggplot2." Hrbrthemes Doc. Available Online Httpsrdrr Iocranhrbrthemes Accessed 26 March 2020.
Salvador Cesa, F., Turra, A., Baruque-Ramos, J., 2017. Synthetic fibers as microplastics in the marine environment: a review from textile perspective with a focus on domestic washings. Sci. Total Environ. 598, 1116–1129. https://doi.org/10.1016/j.scitotenv.2017.04.172.
Salvi, D., Mariottini, P., 2017. Molecular taxonomy in 2D: a novel ITS2 rRNA sequence-structure approach guides the description of the oysters' subfamily Saccostreinae and the genus Magallana (Bivalvia: Ostreidae). Zool. J. Linnean Soc. 179, 263–276.
Sénéchal, N., Gouriou, T., Castelle, B., Parisot, J.-P., Capo, S., Bujan, S., Howa, H., 2009. Morphodynamic response of a meso- to macro-tidal intermediate beach based on a long-term data set. Geomorphology 107, 263–274. https://doi.org/10.1016/j.geomorph.2008.12.016.
Shamskhany, A., Li, Z., Patel, P., Karimpour, S., 2021. Evidence of microplastic size impact on mobility and transport in the marine environment: a review and synthesis of recent research. Front. Mar. Sci. 8, 760649 https://doi.org/10.3389/fmars.2021.760649.
SIBA, 2013. La véritable huître. Dossier de presse. Accessible at. https://www.siba-bassin-arcachon.fr/sites/siba/files/dossier_de_presse_crc_2013.pdf. (Accessed 16 March 2023).

SIBA, 2023. URL. https://geo.bassin-arcachon.com/e-navigation/index.html. (Accessed 27 February 2023).
Suaria, G., Achtypi, A., Perold, V., Lee, J.R., Pierucci, A., Bornman, T.G., Aliani, S., Ryan, P.G., 2020. Microfibers in oceanic surface waters: a global characterization. Sci. Adv. 6, eaay8493. https://doi.org/10.1126/sciadv.aay8493.
Suaria, G., Berta, M., Griffa, A., Molcard, A., Özgökmen, T.M., Zambianchi, E., Aliani, S., 2021. Dynamics of transport, accumulation, and export of plastics at oceanic fronts. In: Belkin, I.M. (Ed.), Chemical Oceanography of Frontal Zones, the Handbook of Environmental Chemistry. Springer, Berlin Heidelberg, Berlin, Heidelberg, pp. 355–405. https://doi.org/10.1007/698_2021_814.
Tapie, N., Budzinski, H., 2018. Quantification de la présence dans les eaux bilan de 2010 à 2016 (Rapport du Reseau Pesticides du Bassin d'Arcachon (REPAR)).
Tata, T., Belabed, B.E., Bououdina, M., Bellucci, S., 2020. Occurrence and characterization of surface sediment microplastics and litter from North African coasts of Mediterranean Sea: preliminary research and first evidence. Sci. Total Environ. 713, 136664 https://doi.org/10.1016/j.scitotenv.2020.136664.
ter Halle, A., Ladirat, L., Martignac, M., Mingotaud, A.F., Boyron, O., Perez, E., 2017. To what extent are microplastics from the open ocean weathered? Environ. Pollut. 227, 167–174. https://doi.org/10.1016/j.envpol.2017.04.051.
TextileExchange, 2022. Preferred Fiber & Materials. Market Report 2021.
Treilles, R., Cayla, A., Gaspéri, J., Strich, B., Ausset, P., Tassin, B., 2020. Impacts of organic matter digestion protocols on synthetic, artificial and natural raw fibers. Sci. Total Environ. 748, 141230 https://doi.org/10.1016/j.scitotenv.2020.141230.
UNEP, 2021. Drowning in Plastics: Marine Litter and Plastic Waste Vital Graphics. United Nations Environment Programme.
Valle-Levinson, A., 2022. Introduction to Estuarine Hydrodynamics, 1st ed. Cambridge University Press. https://doi.org/10.1017/9781108974240.
van Sebille, E., Wilcox, C., Lebreton, L., Maximenko, N., Hardesty, B.D., van Franeker, J. A., Eriksen, M., Siegel, D., Galgani, F., Law, K.L., 2015. A global inventory of small floating plastic debris. Environ. Res. Lett. 10, 124006 https://doi.org/10.1088/1748-9326/10/12/124006.
Wang, T., Zhao, S., Zhu, L., McWilliams, J.C., Galgani, L., Amin, R.M., Nakajima, R., Jiang, W., Chen, M., 2022. Accumulation, transformation and transport of microplastics in estuarine fronts. Nat. Rev. Earth Environ. 3, 795–805. https://doi.org/10.1038/s43017-022-00349-x.
Weis, J.S., De Falco, F., Cocca, M., 2022. Polluting Textiles: The Problem With Microfibres. Routledge.
Wickham, H., 2007. Reshaping data with the reshape package. J. Stat. Softw. 21, 1–20.
Wickham, H., 2016. GGPLOT2: Elegant Graphics for Data Analysis 2016. Springer-Verlag, New York. R Package Version 3.
Wickham, H., Seidel, D., 2020. scales: Scale Functions for Visualization. R Package Version 1, p. 1.
Wickham, H., François, R., Henry, L., Müller, K., 2021. dplyr: A Grammar of Data Manipulation.
WoRMS Editorial Board, 2023. World Register of Marine Species. Available from https://www.marinespecies.org at VLIZ. Accessed 3.13.23. doi:10.14284/170.
Xue, B., Zhang, L., Li, R., Wang, Y., Guo, J., Yu, K., Wang, S., 2020. Underestimated microplastic pollution derived from fishery activities and "hidden" in deep sediment. Environ. Sci. Technol. 54, 2210–2217. https://doi.org/10.1021/acs.est.9b04850.
Zhang, H., 2017. Transport of microplastics in coastal seas. Estuar. Coast. Shelf Sci. 199, 74–86. https://doi.org/10.1016/j.ecss.2017.09.032.
Zhao, S., Zhu, L., Li, D., 2016. Microscopic anthropogenic litter in terrestrial birds from Shanghai, China: not only plastics but also natural fibers. Sci. Total Environ. 550, 1110–1115.